Thermochimica Acta 759 (2026) 180259

Contents lists available at ScienceDirect

Thermochimica Acta

journal homepage: www.elsevier.com/locate/tca

Experimental and Modeling Study of Thermophysical and Excess Properties of 1-Heptanol + Glycol Ether Systems

Khaoula Samadi [a,b], Mohamed Lifi [c,*], Houda Lifi [d], Mohamed Ouakarrouch [d], Fernando Aguilar [a], Fatima Ezzahrae M'hamdi Alaoui [b]

[a] Departamento de Ingeniería Electromecánica, Escuela Politécnica Superior, Universidad de Burgos, 09006 Burgos, Spain
[b] Energy laboratory, Faculty of sciences, University of Abdelmalek Essaadi, Tetouan, Morocco
[c] Department of Mathematics and Computing, Faculty of Science, University of Burgos, 09001 Burgos, Spain
[d] MISCOM Laboratory, National School of Applied Sciences, Cadi Ayyad University, B.P. 46000, Safi, Morocco

ARTICLE INFO

Keywords:
Renewable energy
1-heptanol
Glycol ethers
Redlich-Kister Correlation
Local Composition Models
Predictiv model
Peng−Robinson and PC-SAFT EoS

ABSTRACT

Reducing emissions is a key goal in developing sustainable fuels. Higher alcohols like 1-heptanol play an important key due to their excellent fuel properties, such as high energy content and good combustion behavior, making them promising candidates as renewable fuel additives. This study focuses on the investigation of heat-related behavior of five binary systems composed of glycol ethers with 1-heptanol: diethylene glycol monomethyl ether, diethylene glycol monoethyl ether, ethylene glycol monomethyl ether, ethylene glycol monophenyl ether, and ethylene glycol monobutyl ether. Experimental data were carried out for key thermal and physical properties, including excess molar enthalpy (H_m^E), density (ρ), speed of sound (u), and refractive index (n_D), across the temperature range 293.15–323.15 K at 0.1 MPa. From these primary data, secondary thermophysical properties, namely excess molar volume (V^E), isentropic compressibility (k_s), and refractive index deviation (Δn_D), were derived to better characterize non-ideal mixing behavior. Peng–Robinson and PC-SAFT EOS were using to modeled the density data, while empirical polynomial expressions were applied to fit composition-dependent trends in ρ, u, n_D, and k_s as dependent on fraction. V^E and Δn_D were fitted using the Redlich-Kister equation. The H_m^E was analyzed using both empirical method and heat-related models, including UNIQUAC, NRTL, and the predictive DM-UNIFAC model. All systems exhibited positive H_m^E values, indicating endothermic mixing processes. These findings offer valuable insight into the interaction mechanisms between 1-heptanol and glycol ethers, supporting their evaluation for use in environmentally friendly fuel formulations.

1. Introduction

The urgency of reducing greenhouse gas emissions has grown with the accelerating demand for renewable energy, which created pressure on the transportation sector. To meet climate targets and support sustainable development, minimizing the environmental footprint of transport fuels has become essential [1]. In this context, bio-based fuels have attracted growing interest due to their renewable origin and comparatively lower environmental impact when measured against conventional fossil fuels [2].

For designing cleaner and more efficient fuel blends, biomass-derived oxygenated bio-solvents has been identified as promising renewable alternatives [3]. Their ethers and hydroxyls functional groups, enable them to form strong intermolecular interactions—such as hydrogen bonding and dipole–dipole attractions—particularly with long-chain alcohols like 1-heptanol [4].

A straight-chain primary alcohol, 1-Heptanol, has attracted considerable attention as a viable biofuel additive [5]. Its moderate volatility, hydrophobic character, and favorable energy content make it a valuable component for improving overall fuel performance [6]. Furthermore, its oxygenated structure enhances oxidation pathways during combustion, which helps reduce emissions of carbon monoxide, unburned hydrocarbons, and particulate matter [7].

Characterized with its long aliphatic chain, 1-heptanol shows excellent compatibility with hydrocarbon-based fuels, while its surface-active behavior contributes to better fuel atomization and combustion efficiency. Crucially, since 1-heptanol can be produced from renewable resources through biochemical or catalytic processes, it fits perfectly

* Corresponding author.
E-mail address: mlifi@ubu.es (M. Lifi).

https://doi.org/10.1016/j.tca.2026.180259
Received 23 November 2025; Received in revised form 31 December 2025; Accepted 18 February 2026
Available online 20 February 2026

within the framework of sustainable and green chemistry [8].

Various glycol ethers such as diethylene glycol monomethyl ether, (DEGME); diethylene glycol monoethyl ether, (DEGEE); ethylene glycol monomethyl ether, (EGME); ethylene glycol monophenyl ether, (EGPhE); and ethylene glycol monobutyl ether, (EGBE); play a crucial role as oxygenated fuel additives, effectively reducing emissions such as carbon monoxide and hydrocarbons while enhancing atomization and combustion characteristics in diesel engines [9,10]. Each component contributes distinct properties to the overall fuel mixture [11]. For example, DEGME offers excellent thermal stability thanks to its high boiling point and low volatility, helping to reduce evaporative emissions [12]. In contrast, DEGEE is slightly more hydrophobic, which improves its compatibility with hydrocarbon-based fuels and promotes more uniform combustion [13]. EGME, with its higher volatility and greater oxygen content, enhances cold-start performance and supports efficient combustion, particularly under lower-temperature conditions [14,15]. The presence of an aromatic ring in EGPhE increases its density and reduces volatility, helping to limit evaporation losses while improving the solubility of non-polar fuel components [16,17]. Finally, EGBE strikes a favorable balance between hydrophilic and hydrophobic properties, facilitating well-balanced phase interactions within blended fuel systems [18].

Mixing glycol ethers with 1-heptanol offers a promising approach for developing advanced oxygenated fuels. This combination brings together the favorable volatility and lubricating properties of long-chain alcohols with the emission-reducing and combustion-enhancing characteristics of glycol ethers. As a result, such mixtures can improve fuel atomization, promote cleaner combustion, and enhance cold-start performance in internal combustion engines.

Ongoing research in sustainable energy continues to highlight the importance of thermodynamic evaluation for bio-based fuel systems. Studying key thermophysical properties—such as excess molar enthalpy, density, speed of sound, and refractive index—is essential for gaining deeper insight into fluid behavior and molecular interactions. These measurements not only reveal deviations from ideal mixing but also provide valuable data for developing predictive models and guiding the rational design of more efficient and environmentally friendly fuel formulations.

Among these properties, excess molar enthalpy holds particular significance, as it directly captures the energetic effects of molecular interactions and mixing behavior. When combined with other experimental data, it provides valuable insight into the compatibility of mixture components and supports the optimization of blend formulations. Moreover, thermodynamic models validated through such data offer a reliable framework for predicting system performance across a wide range of operating conditions. This approach helps minimize the need for extensive experimental testing and accelerates the development of next-generation biofuels.

In the current study, we present experimental data for five binary systems involving DEGME (1) + 1-HpOH (2); DEGEE (1) + 1-HpOH (2); EGME (1) +1-HpOH (2); EGPhE (1) + 1-HpOH (2) and EGBE (1) + 1-HpOH (2). Experimental measurements were performed under ambient pressure (0.1 MPa), spanning temperatures from 293.15 K to 323.15 K. The investigated properties include H_m^E, ρ, u, and n_D. Based on these measured properties, several derived heat-related quantities were determined, such as V^E, k_s, and Δn_D. The H_m^E was measured via a quasi-isothermal flow calorimetric technique. The Anton Paar DSA 5000 M densitometer was employed to obtain ρ and u, whereas n_D was determined employing a digital Abbe refractometer. The measured H_m^E values were adjusted using Redlich–Kister equation [19] and analysed with UNIQUAC [20] and NRTL [21] local composition models, and predictive with DM-UNIFAC [22] model, in order to assess their predictive performance and to better understand the intermolecular forces governing these non-ideal mixtures. Polynomial fitting was applied to the experimental measurements of density (ρ), speed of sound (u), refractive index (n_D), and isentropic compressibility (k_s) to establish their correlations. furthermore, the experimental density values were simulated using the Peng–Robinson equation [8] and the PC-SAFT EoS [23].

2. Materials and Methods

The component employed in these experiments: DEGME ($C_5H_{12}O_3$), DEGEE ($C_6H_{14}O_3$), EGME ($C_3H_8O_2$), EGPhE ($C_8H_{10}O_2$), EGBE ($C_6H_{14}O_2$), and 1-HpOH ($C_7H_{16}O$), were obtained from Sigma Aldrich. The water contents of the solvents, as provided by the supplier (Sigma-Aldrich), was performed using a Karl–Fischer coulometric titration (Mettler Toledo C20 coulometric titrator, sensitivity 0.1 μg H_2O) in accordance with ASTM E203 and ISO 760 standards. Before the measurements, all samples were degasified in an ultrasonic bath (Fisher Scientific) to remove any entrained gases and avoid the formation of bubbles during the process that could affect the accuracy of density measurements. No additional purification was performed. The binary systems were prepared gravimetrically using an OHAUS precision balance with an accuracy of ±0.0001 g. Table 1 summarizes the main physical and chemical properties of the compounds studied in this work. A detailed evaluation of the measurement uncertainties for all measured and derived quantities, performed in accordance with the GUM and reported as expanded uncertainties ($k = 2$, 95% confidence level), is provided in the section entitled "Evaluation of Measurement Uncertainties" in the Supplementary Information.

2.1. Excess molar enthalpies

At atmospheric pressure (0.1 MPa), H_m^E were measured using a quasi-isothermal flow calorimetric apparatus (Fig. 1), whose performance has been previously verified in published studies [24]. The experimental setup consisted of two Agilent 1100 HPLC pumps that delivered the pure liquids through chemically resistant stainless-steel tubing into a helical mixing coil housed within a temperature-controlled chamber. A thermostatic circulator maintained the temperature with a precision of ±0.01 K. The mole fractions of the mixtures (x_i) were determined from the flow rate, molar masses, and densities of the pure components, Table 1 reports the densities, ρ, of the measured pure compounds at the delivery temperatures. Different mixture fractions were reached by adjusting the individual flow rates.

The expanded relative uncertainty associated with the excess molar enthalpy measurements was evaluated as ($k = 2$) $Ur\,(H_m^E) = 1\%$, while the uncertainty in the mole fraction (x_i) was within ±0.0005. A detailed uncertainty analysis for H_m^E, conducted according to the EA-4/02 guideline [25], is presented in Table 2.

2.2. Transport properties

Measurements of ρ and u at ambient pressure were performed using an Anton Paar DSA 5000 M vibrating-tube densimeter. The instrument determines density by tracking changes in the oscillation frequency of a U-shaped tube and measures the speed of sound through an ultrasonic pulse-echo technique, ensuring high precision and reproducibility. The combined expanded uncertainties were estimated to be 0.003 g·cm^{-3} for density (ρ) and 1.2 m·s^{-1} for speed of sound (u). Calibration was carried out using standard reference substances—air and deionized water.

Refractive index (n_D) data for both pure substance and pairwise systems were obtained using a digital Abbe-type refractometer (Abbemat 300, Anton Paar). This instrument determines the refractive index based on the deflection of a light beam while passing through the sample. Calibration of the refractometer was also performed with water and air. The expanded relative uncertainty in the refractive index measurements was estimated at ±0.00005 with a 95% confidence level.

Table 1
Purity and chemical data of studied liquids.

Compound	Formula	Molar mass (g/mol)	Density (g/cm^3)		Stated purity[f] (mol%)	Water content[g]	CAS number
			298.15 K	313.15 K			
DEGME*	$C_5H_{12}O_3$	120.15	1.0147[a]	1.0014[a]	>99.0	≤0.03	111-77-3
DEGEE *	$C_6H_{14}O_3$	134.18	0.9852[b]	0.9718[b]	>99.0	≤0.03	111-90-0
EGME*	$C_3H_8O_2$	76.09	0.9598[c]	0.9460[c]	>99.8	≤0.01	109-86-4
EGPhE*	$C_8H_{10}O_2$	138.18	1.1030[d]	1.0900[d]	>99.0	≤0.02	122-99-6
EGBE*	$C_6H_{14}O_2$	118.17	0.89705	0.8863	>99.0	≤0.08	111-76-2
1-HpOH*	$C_7H_{16}O$	116.20	0.81878[e]	0.8080[e]	>99.5	≤0.03	111-70-6

[a] Belhadj et al., [38];
[b] Ouaar et al., [40];
[c] Zarei et al., [43];
[d] Makhlouf et al., [17];
[e] Abala et al., [34].
[f] Purities were provided by the suppliers, and no purification was conducted for the studied compounds.
[g] The water content of the solvents was not measured experimentally in this study but provided by the supplier (Sigma-Aldrich). According to the supplier, the determination was performed using a Karl–Fischer coulometric titration (Mettler Toledo C20 coulometric titrator, sensitivity 0.1 μg H_2O) in accordance with ASTM E203 and ISO 760 standards.
* DEGME: Diethylene glycol monomethyl ether; DEGEE: Diethylene glycol monoethyl ether; EGME: Ethylene glycol monomethyl ether; EGPhE: Ethylene glycol monophenyl ether; and EGBE: Ethylene glycol monobutyl ether; 1-HpOH: 1-heptanol.

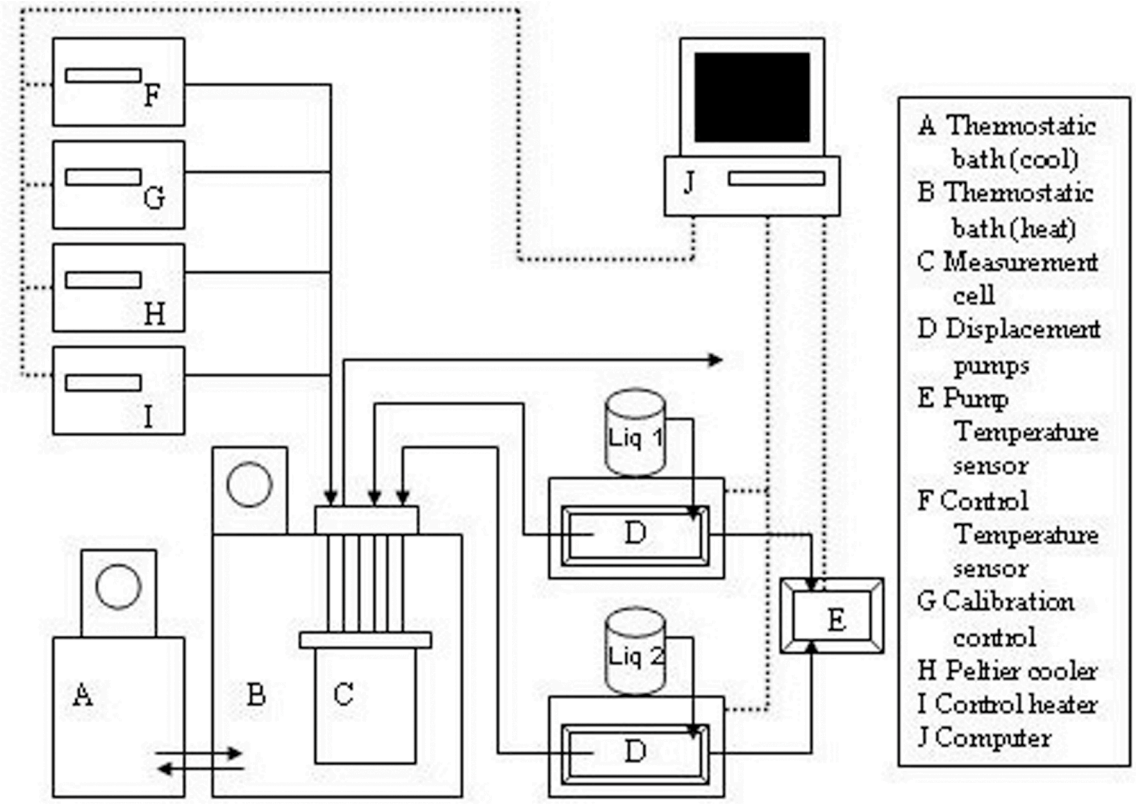

Fig. 1. Quasi-isothermal flow calorimeter. Schematic diagram.

3. Modeling

In this study, several thermodynamic models were employed to report H_m^E and ρ of non-ideal binary systems. UNIQUAC and NRTL models were used to analyze molecular interactions within the mixtures, incorporating the concept of local composition to account for non-random mixing behavior. In addition, the DM-UNIFAC model was applied to predict activity coefficients from the contributions of individual functional groups, providing a practical alternative when experimental data are scarce. For density prediction, two equations of state were utilized: the Peng–Robinson model and the PC-SAFT model. Both are capable of accurately describing the behavior of complex mixtures, especially those involving associating or polar components.

3.1. UNIQUAC model

The non-ideal behavior of liquid mixtures in the UNIQUAC framework is represented by two contributions: combinatorial and residual, where the residual term is formulated as [20]:

$$H_m^E = \sum_{i=1}^{n} q_i x_i \frac{\sum_{j=1}^{n} \vartheta_j \Delta u_{ji} \tau_{ji}}{\sum_{j=1}^{n} \vartheta_j \tau_{ij}} \quad (1)$$

where

Table 2
Uncertainty budget for excess molar enthalpy using EA-4/02 [25][a,b].

		Units	Estimate	Divisor	uncertainty value
$U(Q_{mixture})$	Resolution	W	$4{\cdot}10^{-6}$	$2\sqrt{3}$	$1.15{\cdot}10^{-6}$
$u(Q_{mixture})$	Repeatability		$4{\cdot}10^{-6}$	1	$4{\cdot}10^{-6}$
$u(Q_{mixture})$	Non-linearity		$1.2{\cdot}10^{-4}$	1	$1.2{\cdot}10^{-4}$
$U(\dot{V}_1)$	Accuracy	$cm^3{\cdot}s^{-1}$	$2.5{\cdot}10^{-5}$	2	$1.25{\cdot}10^{-5}$
	Resolution		$1.7{\cdot}10^{-5}$	$2\sqrt{3}$	$7.22{\cdot}10^{-6}$
$U(\dot{V}_2)$	Accuracy	$cm^3{\cdot}s^{-1}$	$2.5{\cdot}10^{-5}$	2	$1.25{\cdot}10^{-5}$
	Resolution		$1.7{\cdot}10^{-5}$	$2\sqrt{3}$	$7.22{\cdot}10^{-6}$
$u(T)$	Stability	K	$1{\cdot}10^{-2}$	1	0.01
$u(H_m^E)$	$H_m^E = 400$	$J{\cdot}mol^{-1}$	N/A	$k = 1$	0.9
$U(H_m^E)$		$J{\cdot}mol^{-1}$	N/A	$k = 2$	1.8
$U_r(H_m^E)$		$J{\cdot}mol^{-1}$/ $J{\cdot}mol^{-1}$	N/A	$k = 2$	$5{\cdot}10^{-3}$

[a] $Q_{mixture}$: heat of mixing; $\dot{V}_1$ and $\dot{V}_2$: flows of pure components 1 and 2 driven by isocratic pumps; T: temperature; H_m^E: excess molar enthalpy; x: mole fraction.
[b] Note that u represents the standard uncertainty, U is the expanded uncertainty with a stated coverage factor of $k = 2$, and U_r is the relative expanded uncertainty with a coverage factor stated in column "Divisor".

$$\vartheta_i = \frac{q_i x_i}{\sum_j q_j x_i} \tag{2}$$

and q_i represents the molecule's surface area, obtained by adding the contributions of the molecule's functional groups.

3.2. NRTL model

NRTL model [21] captures non-idealities in liquid mixtures through the concept of local compositions. The general expression is given by:

$$H_m^E = -RT\sum_{i=1}^{n} x_i \eta_i \tag{3}$$

x_i is the mole fraction of compound i and η_i is is defined as:

$$\eta_i = \frac{\sum_{k=1}^{p} x_k \tau_{ki} G_{ki}\left[\alpha\left(\tau_{ki} - \left(\sum_{n=1}^{p} x_n \tau_{ni} G_{ni} \Big/ \sum_{l=1}^{n} x_l G_{li}\right)\right) - 1\right]}{\sum_{l=1}^{p} x_l G_{li}} \tag{4}$$

α accounts for non-uniformity of molecular forces, thereby enhancing the accuracy of phase equilibrium predictions. In the NRTL framework, G_{ji} is expressed as:

$$G_{ji} = \exp(-\alpha\tau_{ij}) \tag{5}$$

Where

$$\tau_{ij} = (g_{ij} - g_{ii})/RT \tag{6}$$

With, g_{ij} representing the strength of intermolecular forces expressed as energetic interactions between i and j. The NRTL model is particularly well-suited for systems dominated by strong hydrogen bonding.

3.3. DM-UNIFAC model

The DM-UNIFAC model, an extension of UNIQUAC based on group contributions, was employed to predict activity coefficients. The corresponding equation is [22,26].

$$H_m^E = -RT^2\sum_i\sum_k x_i \upsilon_K^{(i)}\left[\left(\frac{\partial \ln\Gamma_K}{\partial T}\right)_{p,x} - \left(\frac{\partial \ln\Gamma_K^{(i)}}{\partial T}\right)_{p,x}\right] \tag{7}$$

$\upsilon_K^{(i)}$ is the number of groups of type k in molecule i. R is the universal gas constant, and T is the absolute temperature.

3.4. PC-SAFT model

PC-SAFT equation of state, originally proposed by Gross and Sadowski [23,27] determines the $\breve{a}^{res}$ as the sum of three contributions:

$$\breve{a}^{res} = \breve{a}^{hc} + \breve{a}^{disp} + \breve{a}^{assoc} \tag{8}$$

Where, $\breve{a}^{hc}$ denotes the hard-chain contribution, a represents the dispersive interactions, and a accounts for specific interactions such as hydrogen bonding. For non-associating components, the model requires three characteristic molecular parameters: the energy's parameter (ε/k), the number of chain segments per molecule (m), and the segment diameter (σ). Associating molecules additionally involve two site-specific parameters: the association energy ($\varepsilon^{A_iB_i}$) and the volume of association (k^{A_iBi}).

In mixtures, using the Lorentz-Berthelot combining rules, the cross-interaction parameters σ_{ij} and ε_{ij} for non-identical segments are determined according to the following expressions:

$$\sigma_{ij} = \left(\frac{\sigma_{ii} + \sigma_{jj}}{2}\right) \tag{9}$$

$$\varepsilon_{ij} = \sqrt{\varepsilon_{ii}\varepsilon_{jj}}\ (1 - k_{ij}) \tag{10}$$

Where, k_{ij} is the interaction coefficient of binary, introduced to correct deviations in unlike interactions. In this work, k was set to zero for all binary systems.

The selected 2B association scheme, which assumes two active sites per molecule, reliably reproduces the densities of the studied liquids. By explicitly considering chain length, molecular size, dispersive forces, and association effects, PC-SAFT provides a comprehensive molecular based framework for modeling thermophysical properties of complex fluids. The theoretical formulation, grounded in statistical thermodynamics [28,29], ensures robust predictions of liquid-phase behavior.

The model parameters were obtained through optimization, minimizing the following objective function:

$$Obj.F = \sum_{i=1}^{M}\left(\frac{\rho_i^{exp} - \rho_i^{calc}}{\rho_i^{exp}}\right)^2 \tag{11}$$

Here, M is the total number of measured densities, ρ_i^{exp} are the experimental densities and ρ_i^{calc} are calculated densities.

3.5. P–R equation

To describe fluid densities, the P-R equation of state expresses the relationship between temperature, pressure, and molar volume, while incorporating non-ideal molecular interactions [8].

$$p = \frac{RT}{\nu - b} - \frac{a(T)}{\nu^2 + 2\nu b - b^2} \tag{12}$$

In this expression, R is the universal gas constant, whereas a and b parameters are substance specific, characterizing attractive forces and excluded volume, respectively. These coefficients are derived from the critical properties of each fluid:

$$b = \frac{0.007780RT_c}{P_c} \tag{13}$$

$$a = a(T_c)\left[1 + k\left(1 - T_c^{0.5}\right)\right]^2 \tag{14}$$

$$a(T_c) = \frac{0.45724R^2T_c^2}{P_c} \tag{15}$$

$$k = 0.37464 + 1.54226\omega - 0.26992\omega^2 \tag{16}$$

Here, P and T denote the critical temperature and critical pressure, respectively. The factor K depends on the acentric factor ω, which is obtained from:

$$\omega = -\log\left(\frac{P}{P_c}\right)_{\frac{T}{T_c}=0.7} - 1 \tag{17}$$

Values of P_c, T_c, and ω for studied compounds were taken from the data base of Yaws [30].

For mixtures, the P-R equation applies the classical van der Waals mixing rules [31] to evaluate the mixture parameters:

$$a_{mix} = \sum_i \sum_j x_i x_j a_{ij} \tag{18}$$

$$b_{mix} = \sum_i x_i b_i \tag{19}$$

with the cross-interaction parameter a_{ij} estimated as:

$$a_{ij} = \left(a_{ii}a_{jj}\right)^2\left(1 - K_{ij}\right) \tag{20}$$

Where, K is the binary interaction coefficient, generally assumed to be zero when no specific data are available, and x_i is the mole fraction of component i.

4. Correlation and fitting

4.1. R-K equation

R-K equation [19] was adopted in this work, as explained:

$$R(x) = x_1.(1 - x_1).\sum_{i=1}^{N} A_i.(2x_1 - 1)^{i-1} \tag{21}$$

In this work, $R(x)$ denotes the general Redlich–Kister polynomial, which can be applied to H_m^E, Δn_D or V^E. The variable x represents the mole composition, while n indicates the number of optimized parameters included in the correlation. The coefficients A_i are affected by reliability of the measurements and the sensitivity of the curve [32]. To establish the appropriate number of terms in the polynomial, Fisher's F-test was employed [33].

4.2. Polynomial adjustment

The experimental ρ, and n_D of each binary mixtures were represented through a general polynomial function expressed as:

$$A(x) = \sum_{i=1}^{N} A_i.x_1^{i-1} \tag{22}$$

Where, $A(x)$ denotes the property under consideration (k_s, u, ρ or n_D); x_1 is the mole composition of the first substance; and A_i are the coefficients of the polynomial correlation obtained through unweighted least-squares fitting procedure.

4.3. Error Analysis parameters

To assess the quality and consistency of the correlated measurement results, a set of statistical parameters was calculated:

- The standard deviation (σ) was determined using:

$$\sigma(X) = \left[\sum_{i=1}^{N} \frac{\left(X_{exp} - X_{calc}\right)^2}{(N - p)}\right]^{1/2} \tag{23}$$

Where, N N is the number of experimental data points, P is the number of fitted parameters, and X_{exp}, X_{calc} correspond to the experimental and calculated values of the property X.

- The Absolute Average Deviation (AAD) is defined as:

$$AAD\ (P) = \frac{100}{N}\sum_{i=1}^{N}\left|\frac{P^E_{m,\ exp} - P^E_{m,\ calc}}{P^E_{exp}}\right| \tag{24}$$

Where, P^E_{exp} and P^E_{calc} denote the experimental and calculated values of property P. Here P may correspond to ρ, H_m^E, n_D, or u.

5. Results and Interpretation

5.1. Thermodynamic properties (H_m^E)

Heat-related properties of pairwise systems comprising glycol ethers with 1-HpOH are strongly affected by the molecular architecture of the components, the nature of intermolecular forces especially temperature variations and hydrogen bonding. Measurement results for the H_m^E of studied mixtures, obtained at both 298.15 K and 313.15 K and at $P = 0.1$ MPa, are illustrated in Fig. 2 and summarized in Tables 3 and 4. The fitted coefficients A_i from the correlation of the H_m^E data using Equation (20) are provided in Table S1 for each binary system. The adjustable parameters in the local composition frameworks to compute H_m^E are compiled in Table S2. Tables 5, 6, 7, and Table S3 include the group volume and surface area parameters [26], the relevant group–group interaction coefficients, structural group classifications, and the calculated average absolute deviations (AAD), respectively for the DM-UNIFAC model. In all mixtures studied, the H_m^E profiles exhibit positive values, confirming an endothermic mixing process. This behavior is mainly explained by the breaking of pronounced self-association via H-bond of the unmixed components and the formation of weaker intermolecular interactions upon mixing dissimilar molecules.

- **General Trends**

All studied binary systems exhibited positive H_m^E values throughout the entire mole-fraction range and studied temperatures, confirming the endothermic nature of mixing. This consistent trend indicates that the required energy to disrupt the self-associative H-bond present in the unmixed components (particularly in 1-HpOH) exceeds the energy released when new hetero-associative interactions form. The growth in H_m^E with temperature reflects the disruption of hydrogen-bonded networks and the enhanced molecular motion, leading to greater deviation from ideality. These effects are particularly strong for glycol ethers with short alkoxy chains, whose structures allow close approach and partial

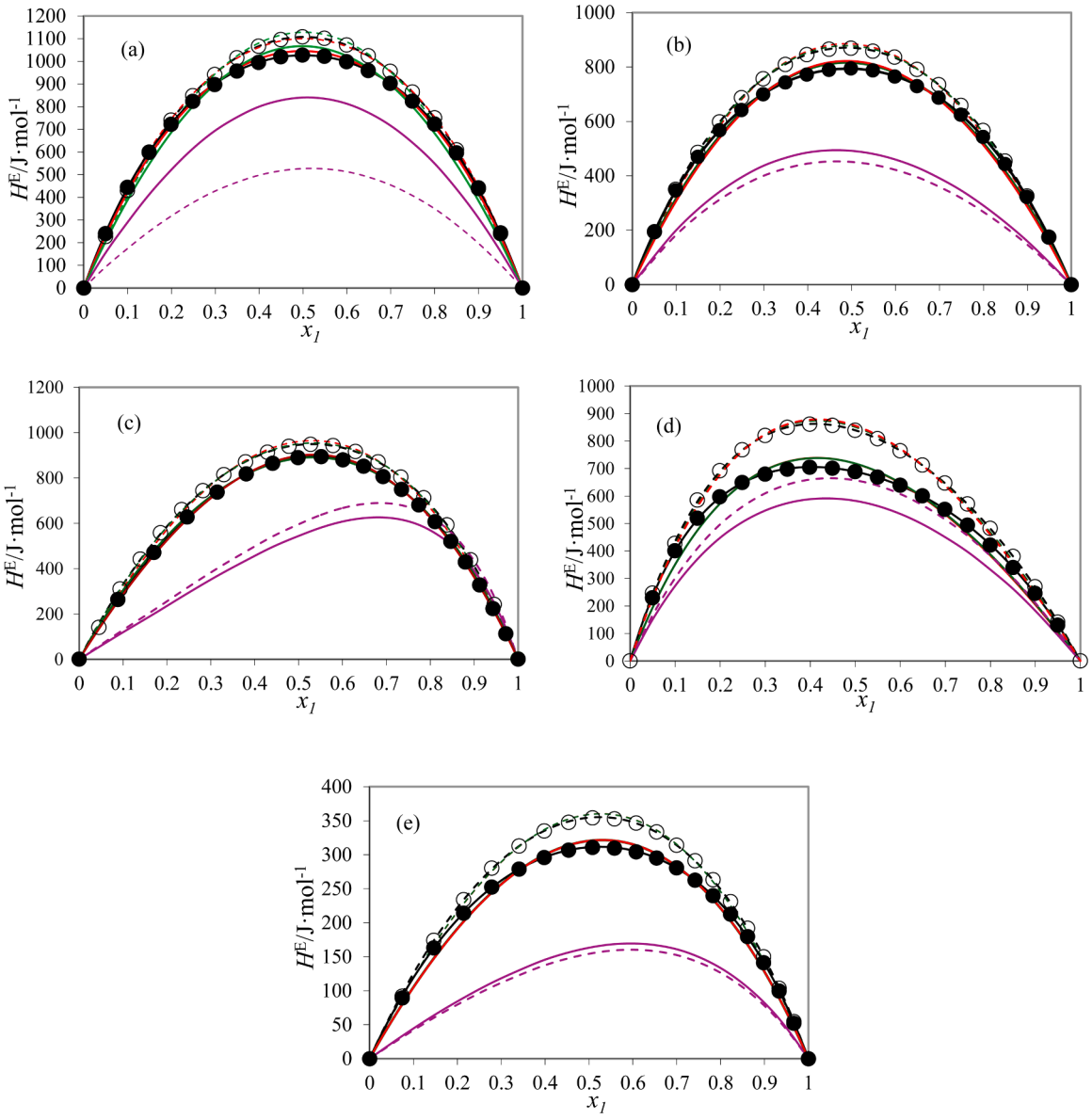

Fig. 2. Excess molar enthalpies, H_m^E, of (a) DEGME + 1-HpOH; (b) DEGEE + 1-HpOH; (c) EGME + 1-HpOH; (d) EGPhE +1-HpOH l and (e) EGBE + 1-HpOH binary mixtures. At T = 298.15 K: ●, experimental data; (——), calculated values with Redlich-Kister (Eq. 21), (——), calculated values with NRTL model (Eq. 3); (——), calculated values with UNIQUAC model (Eq. 1), (——), calculated values with DM-UNIFAC model (Eq. 7). At T = 313.15 K: °, experimental data (- - -), calculated values with Redlich-Kister (Eq. 21), (- - -), calculated values with NRTL model (Eq. 3); (- - -), calculated values with UNIQUAC model (Eq. 1), (- - -), calculated values with DM-UNIFAC model (Eq. 7).

hydrogen bonding but limited packing efficiency with 1-heptanol molecules.

- **Comparative Analysis of Binary Systems**

Short-chain ethers: Among the glycol ethers, DEGME + 1-HpOH and DEGEE + 1-HpOH mixtures exhibit the highest H_m^E magnitudes, with maxima near the equimolar composition. For DEGME + 1-HpOH, H_m^E reaches 1027.6 J·mol^{-1} at 298.15 K and 1108.1 J·mol^{-1} at 313.15 K. This strong endothermic behavior arises from the presence of both hydroxyl and ether groups in DEGME, which enable hydrogen bonding but cannot fully compensate for the strong self-association in unmixed 1-heptanol. Steric hindrance from the flexible glycol chain further prevents efficient molecular packing, resulting in net energy absorption upon mixing.

The DEGEE + 1-HpOH system follows a similar but slightly weaker pattern, with maxima of 795.2 J·mol^{-1} and 869.4 J·mol^{-1} at 298.15 and 313.15 K, respectively. The additional ethyl group in DEGEE reduces polarity and introduces steric constraints, diminishing hydrogen bonding strength. Consequently, the mixture exhibits lower enthalpic deviation than DEGME. Both systems display an increase of H_m^E with temperature, in line with the thermal disruption of hydrogen-bond interactions.

R–K correlation provides the best representation for both systems, followed by NRTL, while UNIQUAC provides a modest underestimation of the peak region. The DM-UNIFAC predictive model reproduces the qualitative behavior but underestimates magnitudes, particularly for DEGEE due to its longer ether chain and increased molecular flexibility.

Intermediate polarity system: The EGME + 1-HpOH mixture displays moderately high H_m^E values, with maxima of 893.4 J·mol^{-1} at 298.15 K and 948.5 J·mol^{-1} at 313.15 K. The curve is slightly asymmetric, reflecting molecular size and polarity differences. EGME's short

Table 3
Experimental data of excess molar enthalpy, H_m^E, of studied mixtures (1) DEGME + 1-HpOH (2); (1) DEGEE + 1-HpOH (2); (1) EGME + 1-HpOH (2); (1) EGPhE +1-HpOH (2) and (1) EGBE + 1-HpOH (2), at T = 298.15 K and P = 0.1 MPa.

x_1	H_m^E/J·mol^{-1}	x_1	H_m^E/J·mol^{-1}	x_1	H_m^E/J·mol^{-1}	x_1	H_m^E/J·mol^{-1}
*x_1 DEGME (1) + (1- x_1) 1-HpOH (2)**							
0.0493	239.8	0.2981	897.2	0.5483	1022.2	0.7993	723.2
0.0995	444.4	0.3488	957.0	0.5987	998.6	0.8491	596.8
0.1488	599.3	0.3985	995.6	0.6482	959.7	0.8992	438.7
0.1989	723.1	0.4489	1020.1	0.6982	902.7	0.9495	243.5
0.2482	823.2	0.4982	1027.6	0.7486	824.2		
*x_1 DEGEE (1) + (1- x_1) 1-HpOH (2)**							
0.0504	193.1	0.2980	700.1	0.5481	788.1	0.7990	543.2
0.0991	347.5	0.3487	743.9	0.5978	765.3	0.8492	443.5
0.1491	470.0	0.3977	772.5	0.6478	730.2	0.8992	322.3
0.1990	567.5	0.4481	790.3	0.6980	687.8	0.9490	175.2
0.2486	642.0	0.4981	790.3	0.7486	625.0		
*x_1 EGME (1) + (1- x_1) 1-HpOH (2)**							
0.0499	148.5	0.2989	586.4	0.5491	638.9	0.7989	389.1
0.0999	276.1	0.3497	623.7	0.5993	611.0	0.8500	304.7
0.1501	382.9	0.3993	646.9	0.6497	571.6	0.8999	212.7
0.1991	466.0	0.4490	657.3	0.6988	523.0	0.9499	110.1
0.2496	535..9	0.4990	655.1	0.7494	460.0		
*x_1 EGPhE (1) + (1- x_1) 1-HpOH (2)**							
0.0499	184.4	0.2981	584.0	0.5479	617.6	0.7991	475.1
0.0991	326.4	0.3491	605.6	0.5986	605.3	0.8494	410.2
0.1494	431.8	0.3979	618.0	0.6487	587.4	0.8989	320.4
0.1990	503.7	0.4476	623.8	0.6980	560.9	0.9492	193.8
0.2481	551.5	0.4980	617.6	0.7483	525.3		
*x_1 EGBE (1) + (1- x_1) 1-HpOH (2)**							
0.0742	89.6	0.3976	296.0	0.6536	295.1	0.8608	179.6
0.1463	163.2	0.4535	306.8	0.6991	280.7	0.8978	141.4
0.2142	214.1	0.5079	310.9	0.7413	262.7	0.9331	99.6
0.2782	252.4	0.5580	309.9	0.7827	239.9	0.9668	52.2
0.3405	278.9	0.6070	304.3	0.8221	212.5		

[a]Standard uncertainties of pressure p, temperature T and mole fraction x are as follows: $u(p)$= 0.001 MPa, $u(T)$ = 0.05 K, $u(x)$ = 0.0005. The relative expanded uncertainty (k = 2) is $U_r(H_m^E)$ = 0.01 for excess molar enthalpy.
* x_1: mole fraction of component 1 (DEGME, DEGEE., EGME., EGPhE.or EGBE.

chain and strong dipolar character allow close molecular contact with 1-heptanol, forming weaker hetero-associative interactions compared to the self-associated hydrogen bonds in the pure liquids.

As temperature rises, increased molecular motion disrupts hydrogen bonds, enhancing endothermicity and deviation from ideality. The R–K equation again provides the best fit, with NRTL and UNIQUAC following. The DM-UNIFAC model captures the positive sign but fails to reproduce the magnitude and asymmetry, due to its simplified treatment of specific interactions.

Bulky or aromatic ethers: The EGPhE + 1-HpOH and EGBE + 1-HpOH systems present lower H_m^Emagnitudes, highlighting the influence of steric hindrance and hydrophobic effects. For EGPhE + 1-HpOH, the maxima reach 623.8 J·mol^{-1} (298.15 K) and 843.9 J·mol^{-1} (313.15 K). The bulky phenyl group restricts hydrogen bonding, while π–π and dispersion interactions play a minor energetic role, resulting in moderate endothermicity. The EGBE + 1-HpOH mixture shows the lowest non-ideality, with maxima of 310.9 J·mol^{-1} at 298.15 K and 352.9 J·mol^{-1} at 313.15 K. The long butyl chain of EGBE introduces significant hydrophobic and steric effects, further reducing the strength and number of hydrogen bonds with 1-heptanol.

For both mixtures, the R–K and NRTL models reproduce experimental results accurately, while UNIQUAC slightly underestimates the maxima. The DM-UNIFAC model captures only qualitative trends, since it cannot explicitly represent π–π or specific hydrogen-bonding interactions.

- **Global Comparison and Interpretation**

Overall, all systems exhibit endothermic mixing with H_m^E increasing with temperature, confirming that hydrogen-bond disruption dominates over dispersion stabilization. The magnitude of H_m^E follows the order:

DEGME > EGME > DEGEE > EGPhE > EGBE

This sequence reflects the combined effects of chain length, polarity, and molecular geometry. Shorter, more polar ethers (DEGME, EGME) produce the strongest deviations from ideality, while longer or aromatic ethers (EGBE, EGPhE) exhibit reduced enthalpic interactions due to steric hindrance and weaker dipolar association. Modeling results consistently confirm that the R–K polynomial is the most reliable correlation method for representing these smooth and symmetric $H_m^E(x_1)$curves, while DM-UNIFAC provides only qualitative predictions. The absence of prior literature data for these five systems underscores the originality and relevance of these measurements.

5.2. volumetric, acoustic, and optical properties

The measured ρ, u and n_D of pairwise systems of: x_1 DEGME + (1- x_1) 1-HpOH; x_1 DEGEE + (1- x_1) 1-HpOH; x_1 EGME + (1- x_1) 1-HpOH; x_1 EGPhE + (1- x_1) 1-HpOH and x_1 EGBE + (1- x_1) 1-HpOH, were carried out at 293.15 K, 303.15 K, 313.15 K and 323.15 K, all at a constant pressure 0.1 MPa. Table 8 summarizes the obtained liquid density data, while their corresponding plots are shown in Fig. 3. The A_i parameters used to fit the density ρ, speed of sound u, and refractive index n_D for each binary mixture, according to Eq. (22), are provided in Table S4. PC-SAFT EoS parameters for the studied substances are reported in Table 9, whereas Table 10 summarizes the corresponding P–R EoS parameters

Table 4
Experimental data of excess molar enthalpy, H_m^E, of studied mixtures (1) DEGME + 1-HpOH (2); (1) DEGEE + 1-HpOH (2); (1) EGME + 1-HpOH (2); (1) EGPhE +1-HpOH (2) and (1) EGBE + 1-HpOH (2), at T = 313.15 K and P = 0.1 MPa.

x_1	H_m^E/J·mol^{-1}	x_1	H_m^E/J·mol^{-1}	x_1	H_m^E/J·mol^{-1}	x_1	H_m^E/J·mol^{-1}
*x_1 DEGME (1) + (1- x_1) 1-HpOH (2)**							
0.0493	227.6	0.2981	942.4	0.5483	1101.4	0.7993	750.4
0.0995	429.9	0.3488	1016.2	0.5987	1072.3	0.8491	609.8
0.1487	598.6	0.3985	1067.3	0.6482	1024.2	0.8992	442.3
0.1989	741.5	0.4488	1095.8	0.6982	956.4	0.9495	240.3
0.2482	848.8	0.4983	1108.1	0.7486	864.7		
*x_1 DEGEE (1) + (1- x_1) 1-HpOH (2)**							
0.0504	195.1	0.2980	757.0	0.5481	858.9	0.7990	566.6
0.0991	350.8	0.3487	809.5	0.5977	836.5	0.8492	454.9
0.1491	486.6	0.3978	845.6	0.6487	792.0	0.8992	325.8
0.1989	598.7	0.4480	865.5	0.6980	735.6	0.9490	175.1
0.2486	687.6	0.4981	869.4	0.7486	659.4		
*x_1 EGME (1) + (1- x_1) 1-HpOH (2)**							
0.0451	140.9	0.2821	744.2	0.5276	948.5	0.7851	712.4
0.0932	310.7	0.3300	814.1	0.5786	942.4	0.8378	593.2
0.1392	441.9	0.3790	870.7	0.6295	916.9	0.8917	438.0
0.1855	558.4	0.4291	913.0	0.6812	870.9	0.9459	241.5
0.2339	660.0	0.4781	939.0	0.7332	804.0		
*x_1 EGPhE (1) + (1- x_1) 1-HpOH (2)**							
0.0498	203.0	0.2981	760.4	0.5480	835.1	0.7991	607.3
0.0991	375.4	0.3491	803.0	0.5986	815.6	0.8494	509.4
0.1494	510.2	0.3979	827.9	0.6487	784.9	0.8989	384.7
0.1991	619.3	0.4476	842.6	0.6981	741.7	0.9492	219.7
0.2482	701.1	0.4981	843.9	0.7483	683.8		
*x_1 EGBE (1) + (1- x_1) 1-HpOH (2)**							
0.0742	92.1	0.3976	335.0	0.6536	333.8	0.8608	192.2
0.1462	174.3	0.4534	347.6	0.6991	314.1	0.8977	150.0
0.2141	234.0	0.5078	354.2	0.7412	291.1	0.9330	103.7
0.2782	280.5	0.5580	352.9	0.7826	263.4	0.9668	54.7
0.3404	312.9	0.6070	346.6	0.8221	231.0		

[a]Standard uncertainties of pressure p, temperature T and mole fraction x are as follows: $u(p)$= 0.001 MPa, $u(T)$ = 0.05 K, $u(x)$ = 0.0005. The relative expanded uncertainty (k = 2) is $U_r(H_m^E)$ = 0.01 for excess molar enthalpy.
* x_1: mole fraction of component 1 (DEGME, DEGEE., EGME., EGPhE.or EGBE).

Table 5
DM-UNIFAC relative Van der Waals volumes R_K and surface areas Q_K [26].

Main group	Subgroup	R_K	Q_K
CH_2	CH_3	0.6325	1.0608
	CH_2	0.6325	0.7081
OH	OH	1.2302	0.8927
CH_2O	CH_3O	1.1434	1.6022
	CH_2O	1.1434	1.2495
	CHO	1.1434	0.8968
ACOH	ACOH	1.080	0.9750

Table 6
DM-UNIFAC group interaction parameters used in this work.

Main group		Group interaction parameters		
1	2	a_{12}/K	b_{12}/K	c_{12}/K^{-1}
		a_{21}/K	b_{21}/K	c_{21}/K^{-1}
CH_2	OH	2777	-4.674	0.001551
		1606	-4.746	0.0009181
CH_2	CH_2O	233.1	-0.3155	-
		-9.654	-0.03242	-
CH_2	ACOH	1381	-0.9977	-
		1987	-4.615	-
OH	CH_2O	816.7	-5.092	0.00606
		650.9	-0.7132	0.000815
OH	ACOH	83.91	-1.262	-
		465.4	-1.841	-

[29].

- **Density, (ρ)**

As temperature increases, all the measured density decreases consistently, which is characteristic of the thermal expansion behavior of liquids. This behavior reflects the dominance of physical contributions, namely increased molecular spacing and reduced packing efficiency as thermal motion intensifies. The smooth and continuous variation of density with composition further confirms complete miscibility and the absence of phase separation, indicating gradual structural reorganization of the liquid mixtures [34,35].

From a molecular standpoint, the density behavior results from the competition between physical and chemical effects. The physical contribution arises from size and shape differences between glycol ethers and 1-HpOH, which influence free volume and packing efficiency. In contrast, the chemical contribution originates from specific interactions, mainly hydrogen bonding between the hydroxyl group of 1-HpOH and ether oxygen atoms. These interactions promote local structuring and partial contraction of the liquid phase, partially counteracting thermal expansion effects, particularly in ether-rich or strongly associating mixtures [34].

Among the tested correlations, the polynomial model shows the best agreement with the experimental density values, reflecting the flexibility of its empirical formulation. However, PC-SAFT equation shows a generally good predictive performance, with noticeably better accuracy at higher pressures. At atmospheric pressure, it tends to underestimate

Table 7
Molecular formulae of the species in this work, shown as structures of subgroups for group-contribution models.

Component	Structure	Molecular formula
2-(2-methoxyethoxy) ethanol	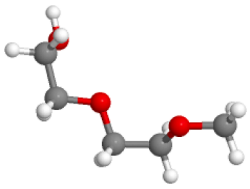	CH_3O- CH_2- CH_2O- CH_2- CH_2-OH
2-(2-ethoxyethoxy) ethanol	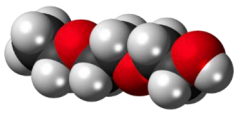	CH_3- CH_2O- CH_2- CH2O- CH_2 - CH_2-OH
2-methoxyethanol	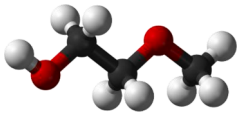	CH_3O-CH_2- CH_2-OH
2-phenoxyethanol	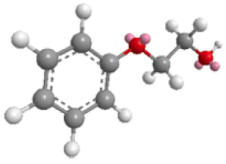	C_6H_5O- CH_2- CH_2-OH
2-butoxyethanol	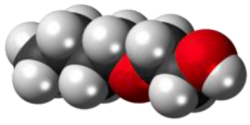	CH_3-$(CH_2)_2$-CH_2O- CH_2-CH_2-OH
1-heptanol	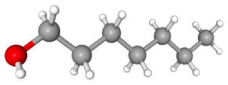	CH_3- CH_2-CH_2-CH_2- CH_2-CH_2-CH_2-OH

the liquid density, especially in mixtures rich in 1-HpOH. This suggests that the model has some limitations in capturing strong hydrogen-bonding effects under low-pressure conditions. Although PC-SAFT includes an association term to represent these interactions, its simplified treatment may not fully describe the extensive self-association typical of long-chain alcohols such as 1-HpOH. These observations are consistent with the results reported by [36] for the DBE + 1-heptanol system, where PC-SAFT showed improved agreement with experimental density data at high pressure, while underestimating densities near atmospheric conditions. Their findings confirm that the predictive performance of PC-SAFT is enhanced as pressure increases, due to the reduced influence of specific interactions under compression.

In contrast, the PR equation shows the poorest performance among all the models. At atmospheric pressure, it consistently underestimates the liquid density across the entire composition range, with larger deviations appearing in alcohol-rich mixtures. This behavior is expected since the PR equation, originally developed for non-polar or weakly interacting systems, does not include explicit terms to describe molecular association. As a result, it fails to accurately represent the strong hydrogen bonding found in 1-HpOH and ether–alcohol mixtures. Although its cubic form makes it computationally simple, it cannot capture the molecular-level interactions that govern the structure of polar or associating liquids.

- **Speed of sound, *(u)***

Across all binary systems, u demonstrates an nonlinear trend with composition, showing either maxima or minima at intermediate mole

Table 8
Densities, ρ, speed of sound, u, and refractive indices, n_D, for the binarys ystems {(1) DEGME + 1-HpOH (2); (1) DEGEE + 1-HpOH (2); (1) EGME + 1-HpOH (2); (1) EGPhE +1-HpOH (2) and (1) EGBE + 1-HpOH (2)} at T = (293.15, 303.15, 313.15 and 323.15) K and at P = 0.1MPa.

x_1	ρ /(10^3g.cm^{-3})	u/(m.s^{-1})	ks (10^{12} Pa^{-1})	n_D
{DEGME (1) + 1-HpOH (2)}				
T = 293.15 K				
0.0000	0.8222	1344.18	673.12	1.4244
0.1039	0.8393	1345.77	657.83	1.4239
0.1929	0.8552	1348.09	643.40	1.4236
0.3006	0.8721	1351.74	627.55	1.4236
0.4029	0.8892	1356.86	610.84	1.4234
0.5044	0.9084	1363.76	591.93	1.4236
0.6060	0.9299	1373.33	570.17	1.4239
0.7002	0.9505	1384.33	549.02	1.4242
0.7965	0.9718	1397.79	526.65	1.4247
0.8945	0.9952	1414.09	502.52	1.4254
1.0000	1.0213	1435.1	475.41	1.4262
T = 303.15 K				
0.0000	0.814088	1310.68	715.05	1.4205
0.1039	0.831812	1310.7	699.79	1.4200
0.1929	0.848109	1314.69	682.18	1.4196
0.3006	0.864979	1318.44	665.08	1.4196
0.4029	0.881728	1323.54	647.43	1.4195
0.5044	0.90059	1330.46	627.29	1.4197
0.6060	0.921801	1339.89	604.26	1.4200
0.7002	0.942579	1351.09	581.18	1.4203
0.7965	0.96395	1364.34	557.31	1.4208
0.8945	0.986572	1380.56	531.82	1.4214
1.0000	1.012795	1403.27	501.41	1.4223
T = 313.15 K				
0.0000	0.807891	1277.29	758.70	1.4165
0.1039	0.824956	1278.75	741.31	1.4160
0.1929	0.840737	1281.48	724.30	1.4157
0.3006	0.857369	1284.96	706.40	1.4155
0.4029	0.87398	1290.27	687.29	1.4156
0.5044	0.892666	1296.98	665.95	1.4156
0.6060	0.913845	1306.9	640.68	1.4159
0.7002	0.934288	1317.63	616.50	1.4162
0.7965	0.955339	1331.04	590.83	1.4168
0.8945	0.977885	1346.99	563.62	1.4175
1.0000	1.003819	1368.31	532.08	1.4184
T = 323.15 K				
0.0000	0.800874	1244.13	806.69	1.4125
0.1039	0.817562	1246.11	787.71	1.4120
0.1929	0.833134	1248.71	769.77	1.4118
0.3006	0.849279	1252.36	750.74	1.4116
0.4029	0.866004	1257.54	730.19	1.4116
0.5044	0.88471	1264.48	706.93	1.4117
0.6060	0.905582	1274.15	680.19	1.4120
0.7002	0.92587	1284.71	654.39	1.4123
0.7965	0.946838	1298.08	626.79	1.4129
0.8945	0.969124	1313.63	597.96	1.4135
1.0000	0.994865	1334.64	564.30	1.4144
{DEGEE (1) + 1-HpOH (2)}				
T = 293.15 K				
0.0000	0.8222	1344.18	673.12	1.4244
0.1023	0.8385	1344.46	659.81	1.4243
0.2006	0.8534	1345.39	647.34	1.4242
0.2985	0.8691	1347.46	633.72	1.4243
0.4047	0.8848	1350.34	619.79	1.4245
0.5012	0.9017	1354.45	604.53	1.4248
0.5994	0.9185	1359.51	589.07	1.4251
0.6903	0.9349	1366.31	572.96	1.4256
0.7905	0.9521	1373.68	556.61	1.4261
0.9016	0.9693	1382.83	539.50	1.4267
1.0000	0.9886	1394.02	520.52	1.4273
T = 303.15 K				
0.0000	0.8141	1310.68	715.05	1.4205
0.1023	0.8313	1310.88	700.06	1.4203
0.2006	0.8461	1311.86	686.80	1.4202
0.2985	0.8615	1313.83	672.45	1.4203
0.4047	0.8772	1316.76	657.47	1.4205

(*continued on next page*)

Table 8 (*continued*)

x_1	ρ /(10^3g.cm^{-3})	u/(m.s^{-1})	ks (10^{12} Pa^{-1})	n_D
0.5012	0.8937	1320.68	641.50	1.4207
0.5994	0.9106	1326.02	624.54	1.4210
0.6903	0.9272	1332.28	607.62	1.4215
0.7905	0.9436	1339.38	590.75	1.4220
0.9016	0.9606	1348.18	572.72	1.4225
1.0000	0.9797	1359.04	552.61	1.4229
$T = 313.15$ K				
0.0000	0.8079	1277.29	758.70	1.4165
0.1023	0.8240	1277.49	743.64	1.4164
0.2006	0.8386	1278.35	729.71	1.4163
0.2985	0.8539	1280.22	714.55	1.4162
0.4047	0.8693	1282.99	698.82	1.4164
0.5012	0.8858	1286.82	681.78	1.4167
0.5994	0.9022	1292.53	663.48	1.4170
0.6903	0.9185	1297.83	646.36	1.4174
0.7905	0.9352	1305.06	627.83	1.4179
0.9016	0.9520	1313.62	608.75	1.4183
1.0000	0.9708	1324.1	587.53	1.4186
$T = 323.15$ K				
0.0000	0.8009	1244.13	806.69	1.4125
0.1023	0.8166	1244.43	790.79	1.4123
0.2006	0.8310	1245.46	775.77	1.4122
0.2985	0.8461	1247.2	759.81	1.4121
0.4047	0.8614	1249.98	743.00	1.4123
0.5012	0.8777	1253.78	724.82	1.4126
0.5994	0.8939	1258.4	706.46	1.4129
0.6903	0.9101	1264.3	687.43	1.4133
0.7905	0.9265	1271.25	667.89	1.4138
0.9016	0.9432	1279.66	647.48	1.4144
1.0000	0.9618	1289.49	625.30	1.4143
{EGME (1) + 1-HpOH (2)}				
$T = 293.15$ K				
0.0000	0.8222	1344.18	673.12	1.4244
0.1014	0.8301	1341.11	669.83	1.4226
0.2008	0.8383	1337.76	666.56	1.4208
0.3031	0.8479	1334.9	661.88	1.4188
0.4030	0.8584	1332.92	655.72	1.4167
0.5019	0.8702	1331.71	648.00	1.4147
0.6034	0.8840	1331.88	637.69	1.4125
0.7031	0.8994	1333.89	624.86	1.4100
0.8015	0.9178	1338.47	608.20	1.4076
0.9015	0.9394	1347.35	586.41	1.4049
1.0000	0.9647	1360.37	560.16	1.4024
$T = 303.15$ K				
0.0000	0.8141	1310.68	715.05	1.4205
0.1014	0.8222	1307.45	711.51	1.4186
0.2008	0.8306	1303.91	708.12	1.4169
0.3031	0.8404	1301.46	702.54	1.4147
0.4030	0.8507	1299.25	696.37	1.4128
0.5019	0.8623	1298.08	688.23	1.4106
0.6034	0.8759	1298.09	677.52	1.4084
0.7031	0.8912	1300.1	663.86	1.4059
0.8015	0.9092	1304.66	646.16	1.4036
0.9015	0.9306	1313.17	623.18	1.4008
1.0000	0.9556	1325.78	595.34	1.3983
$T = 313.15$ K				
0.0000	0.8079	1277.29	758.70	1.4165
0.1014	0.8156	1274.06	755.34	1.4146
0.2008	0.8236	1270.86	751.81	1.4129
0.3031	0.8328	1267.97	746.90	1.4107
0.4030	0.8429	1265.78	740.47	1.4088
0.5019	0.8543	1264.36	732.23	1.4066
0.6034	0.8677	1264.64	720.58	1.4044
0.7031	0.8828	1266.34	706.36	1.4019
0.8015	0.9005	1270.78	687.63	1.3995
0.9015	0.9216	1279.03	663.25	1.3968
1.0000	0.9463	1291.09	633.95	1.3942
$T = 323.15$ K				
0.0000	0.8009	1244.13	806.69	1.4125
0.1014	0.8082	1240.91	803.52	1.4106
0.2008	0.8157	1237.77	800.21	1.4088
0.3031	0.8250	1234.7	795.08	1.4067
0.4030	0.8350	1232.41	788.53	1.4047
0.5019	0.8462	1231.12	779.69	1.4027
0.6034	0.8594	1231.09	767.76	1.4006
0.7031	0.8743	1232.49	752.93	1.3982
0.8015	0.8917	1236.63	733.33	1.3953
0.9015	0.9125	1238.34	714.60	1.3927
1.0000	0.9367	1255.74	677.00	1.3901
{EGPhE (1) + 1-HpOH (2)}				
$T = 293.15$ K				
0.0000	0.8222	1344.18	673.12	1.4244
0.1058	0.8489	1360.68	636.28	1.4350
0.2020	0.8740	1376.87	603.53	1.4450
0.3010	0.9005	1395.25	570.46	1.4555
0.3978	0.9270	1415.15	538.67	1.4661
0.4950	0.9542	1437.16	507.39	1.4768
0.6012	0.9848	1464.1	473.70	1.4893
0.6974	1.0132	1490.8	444.07	1.5005
0.7972	1.0434	1521.41	414.04	1.5130
0.8931	1.0732	1553.07	386.31	1.5250
1.0000	1.1072	1591.29	356.66	1.5387
$T = 303.15$ K				
0.0000	0.8222	1310.68	707.97	1.4205
0.1058	0.8489	1327.24	668.74	1.4186
0.2020	0.8667	1343.63	639.09	1.4169
0.3010	0.8930	1362.03	603.64	1.4147
0.3978	0.9193	1382.24	569.34	1.4128
0.4950	0.9464	1404.43	535.69	1.4106
0.6012	0.9769	1431.04	499.87	1.4084
0.6974	1.0052	1457.6	468.25	1.4059
0.7972	1.0352	1487.83	436.38	1.4036
0.8931	1.0648	1519.24	406.88	1.4008
1.0000	1.0987	1556.67	375.59	1.3983
$T = 313.15$ K				
0.0000	0.8079	1277.29	758.70	1.4165
0.1058	0.8347	1293.95	715.56	1.4146
0.2020	0.8595	1310.44	677.53	1.4129
0.3010	0.8855	1329.03	639.35	1.4107
0.3978	0.9116	1349.33	602.48	1.4088
0.4950	0.9385	1371.17	566.71	1.4066
0.6012	0.9688	1397.94	528.18	1.4044
0.6974	0.9969	1424.58	494.27	1.4019
0.7972	1.0268	1454.37	460.42	1.3995
0.8931	1.0563	1485.48	429.02	1.3968
1.0000	1.0901	1522.58	395.71	1.3942
$T = 323.15$ K				
0.0000	0.8009	1244.13	806.69	1.4125
0.1058	0.8273	1261.23	759.91	1.4106
0.2020	0.8519	1277.91	718.80	1.4088
0.3010	0.8778	1296.87	677.35	1.4067
0.3978	0.9038	1317.06	637.84	1.4047
0.4950	0.9307	1338.88	599.40	1.4027
0.6012	0.9608	1365.62	558.10	1.4006
0.6974	0.9888	1392.05	521.90	1.3982
0.7972	1.0185	1421.56	485.84	1.3953
0.8931	1.0479	1452.33	452.43	1.3927
1.0000	1.0815	1488.64	417.25	1.3901
{EGBE (1) + 1-HpOH (2)}				
$T = 293.15$ K				
0.0000	0.8222	1344.18	673.12	1.4244
0.1008	0.8297	1341.34	669.85	1.4237
0.2049	0.8375	1338.49	666.46	1.4232
0.3046	0.8452	1335.75	663.15	1.4226
0.4014	0.8527	1333.63	659.37	1.4221
0.5034	0.8609	1331.55	655.17	1.4217
0.6020	0.8688	1329.75	650.91	1.4213
0.7036	0.8772	1328.46	645.94	1.4208
0.8027	0.8855	1327.37	640.94	1.4204
0.9002	0.8938	1326.73	635.61	1.4200
1.0000	0.9025	1325.7	630.49	1.4197
$T = 303.15$ K				
0.0000	0.8141	1310.68	715.05	1.4205
0.1008	0.8226	1307.89	710.67	1.4198
0.2049	0.8302	1304.89	707.37	1.4192
0.3046	0.8377	1302.34	703.80	1.4186
0.4014	0.8452	1300.12	699.99	1.4181

(*continued on next page*)

Table 8 (*continued*)

x_1	ρ /(10^3g.cm^{-3})	u/(m.s^{-1})	ks (10^{12} Pa^{-1})	n_D
0.5034	0.8532	1298.14	695.49	1.4176
0.6020	0.8611	1296.39	690.97	1.4171
0.7036	0.8695	1294.78	686.00	1.4167
0.8027	0.8779	1293.8	680.49	1.4162
0.9002	0.8862	1293.02	674.90	1.4159
1.0000	0.8950	1291.77	669.60	1.4155
T = 313.15 K				
0.0000	0.8079	1277.29	758.70	1.4165
0.1008	0.8152	1274.53	755.12	1.4158
0.2049	0.8228	1271.48	751.73	1.4151
0.3046	0.8302	1268.86	748.16	1.4146
0.4014	0.8375	1266.52	744.38	1.4140
0.5034	0.8454	1264.61	739.65	1.4134
0.6020	0.8532	1262.64	735.19	1.4130
0.7036	0.8614	1261.19	729.81	1.4125
0.8027	0.8697	1260.1	724.16	1.4121
0.9002	0.8779	1259.21	718.41	1.4117
1.0000	0.8863	1257.69	713.31	1.4113
T = 323.15 K				
0.0000	0.8009	1244.13	806.69	1.4125
0.1008	0.8080	1241.32	803.24	1.4118
0.2049	0.8153	1238.35	799.80	1.4111
0.3046	0.8225	1235.71	796.18	1.4104
0.4014	0.8296	1233.29	792.46	1.4099
0.5034	0.8454	1231.3	780.21	1.4093
0.6020	0.8452	1229.28	782.95	1.4087
0.7036	0.8532	1227.72	777.55	1.4082
0.8027	0.8613	1226.18	772.20	1.4078
0.9002	0.8693	1225.44	766.02	1.4074
1.0000	0.8776	1223.92	760.64	1.4070

[a] Standard uncertainties of pressure p, temperature T, are as follows: $u(p)$= 0.004 MPa, $u(T)$ = 0.02 K. The expanded uncertainty of mole fraction x is $U(x)$= 0.0008. The combined expanded uncertainties U_c in density ρ, speed of sound u, and refractive index n_D are as follow: $U_c(\rho) = 0.003$ g·cm^{-3}, $U_c(u) = 1.2$ m·s^{-1}, and $U_c(n_D) = 0.005$, with a 0.95 level of confidence.

fractions, as shown in Fig. 4. The observed non-ideal behavior highlights strong intermolecular interactions between the mixture's components, mainly due to hydrogen bonding and dipole–dipole forces typical features of systems containing alcohols and ethers.

The observed deviations can be interpreted as follows: the physical contribution is related to changes in density and adiabatic compressibility caused by molecular size mismatch and packing rearrangements. Simultaneously, the chemical contribution, dominated by hydrogen bonding and dipole–dipole interactions between glycol ethers and 1-HpOH, leads to the formation and disruption of transient molecular complexes. These complexes modify the liquid structure and directly affect compressibility, thereby influencing acoustic propagation [37].

The speed of sound decreases systematically for all mixtures, as the temperature increases from 293.15 K to 323.15 K. This trend indicates that higher temperatures weaken the intermolecular cohesion, as the increased molecular motion overcomes the attractive forces between molecules. The reduction in sound velocity with temperature is consistent with the accompanying decrease in density and the rise in compressibility, which are typical behaviors of associating liquids.

DEGME and EGME, containing more hydrophilic glycol ethers, shows more pronounced deviations from ideal behavior. This suggests stronger hydrogen bonding or molecular association effects in these mixtures compared to those with more bulky or hydrophobic substituents.

An excellent agreement was observed using the polynomial correlation to fit the experimental data, as indicated by the close overlap among the measured points and theoretical plots. This confirms the reliability of the applied model in describing how acoustic properties vary with composition and temperature. Such consistent correlations are particularly useful for predicting the behavior of related systems and for gaining deeper insight into the thermodynamic properties governed by molecular interactions in mixed components.

- **Refractive index, (n_D)**

It is well established that the refractive index of an ideal solution is not a simple mole-fraction weighted average of the pure-component refractive indices; instead, volume-fraction–based mixing rules are known to provide close agreement with experimental values. The results were illustrated in Fig. 5 at four temperatures, reflecting the sensitivity of optical properties to both molecular polarizability and specific intermolecular interactions.

Among all systems, DEGME + 1-HpOH exhibits the highest refractive index values and the most pronounced non-linearity across the composition range. This behavior is attributed to the combined effect of high molecular polarizability due to multiple ether groups and strong hydrogen bonding with 1-HpOH. The DEGEE + 1-HpOH system shows a similar but less pronounced trend, as the substitution of a methyl group with an ethyl group reduces overall polarity and interaction strength [35].

From a physical standpoint, the refractive index is strongly governed by electronic polarizability, which depends on molecular size, functional groups, and the presence of aromatic rings. Systems containing DEGME show the highest refractive index values and the strongest curvature over the entire composition range. This behavior is attributed to the presence of two ether oxygen atoms, which enhance molecular polarizability, leading to increased optical density of the mixture. DEGEE + 1-HpOH displays a similar but less pronounced trend, as the substitution of a methyl group by an ethyl group slightly reduces polarity and polarizability.

The chemical contribution becomes evident through hydrogen bonding between the hydroxyl group of 1-heptanol and the ether oxygen atoms. These specific interactions lead to local structuring and changes in electronic environments, which amplify deviations from linearity in nD. Such effects are particularly pronounced in mixtures containing more hydrophilic glycol ethers, where stronger association enhances the refractive response.

The mixture containing EGME shows an intermediate trend, with moderate refractive index values and smoother curvature, consistent with its simpler structure featuring only one ether group. In contrast, the EGPhE + 1-HpOH system exhibits higher refractive indices, especially at greater mole fractions of the ether component. This can be attributed to the aromatic ring, which enhances molecular polarizability through delocalized π-electrons.

Finally, the EGBE mixture displays the lowest refractive indices and behaves closest to an ideal system, as the longer butyl chain diminishes overall polarity and intermolecular attraction.

Overall, the refractive index results clearly demonstrate that molecular structure—ether functionality, aromaticity, and alkyl chain length—controls the balance between physical and chemical contributions in these binary mixtures. This interpretation is fully consistent with recent literature, where refractive index deviations have been successfully employed to discriminate between structural packing effects and specific intermolecular interactions in associating liquid systems.

- **Comparison with literature data**

The thermal and physical properties measured for the pure compounds in this study were examined in light of reliable literature data [15,17,36,38–46], and an overall excellent agreement was observed. In terms of density, 1-HpOH showed particularly close consistency with published values, displaying the lowest AAD of 0.01% at 293.15 K (with Abala et al. [36]; Alaoui et al. [39]) and a maximum deviation of 0.14% at 303.15 K (with Pina and Francesconi [44]) and 0.09% at 313.15 K (with Aralaguppi and Baragi [40]). Comparable accuracy was achieved for the other pure compounds, with minimal deviations overall. The

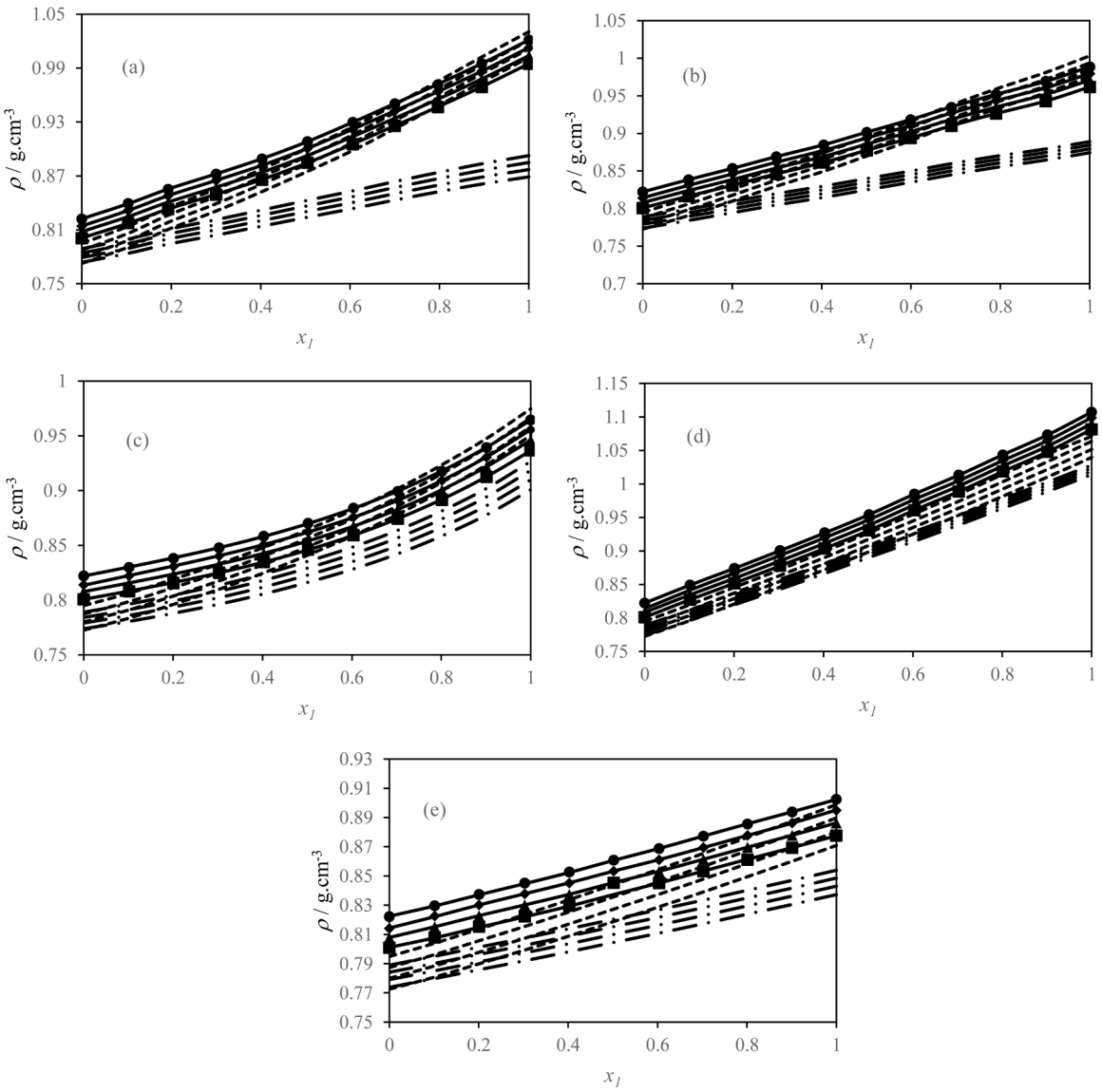

Fig. 3. Experimental values of densities, ρ, for the binary mixture (a) DEGME + 1-HpOH; (b) DEGEE + 1-HpOH; (c) EGME + 1-HpOH; (d) EGPhE +1-HpOH l and (e) EGBE + 1-HpOH, where: ●, 293.15 K; ◊, 303.15 K; ▲, 313.15 K; □, 323.15 K. (solid line) polynomial equation, (dotted line) PC-SAFT equation (Eq. 8), (dashed line) Peng−Robinson equation (Eq. 12).

Table 9
PC-SAFT parameters for the pure compounds considered in this work.

Compound *	m[-]	σ [A]	ε/K [K]	ε^{AB}/K [K]	K^{AB}	AAD %
DEGME	5.3913	3.10393	227.797	1920.95	0.0327234	$1.65{\cdot}10^{-4}$
DEGEE	5.74342	3.18681	230.644	1544.38	0.0358667	$2.00{\cdot}10^{-4}$
EGME	4.98311	2.82126	266.361	1792.03	0.0135779	$4.54{\cdot}10^{-6}$
EGPhE	3.8767	3.52531	200.01	3000	0.0752282	$7.00{\cdot}10^{-2}$
EGBE	3.93576	3.55106	210.06	2927.62	0.069592	$1.33{\cdot}10^{-5}$
1-HpOH	4.67716	3.5136	272.198	2318.74	0.04	$5.00{\cdot}10^{-2}$

* DEGME: Diethylene glycol monomethyl ether; DEGEE: Diethylene glycol monoethyl ether; EGME: Ethylene glycol monomethyl ether; EGPhE: Ethylene glycol monophenyl ether; and EGBE: Ethylene glycol monobutyl ether.

smallest density discrepancies were found for EGME (with Zarei et al. [46]) and EGPhE (with Makhlouf et al. [17]), both with AADs around 0.02% at 293.15 K, while the largest difference, 0.30% at 303.15 K, corresponded to EGBE (with Dubey and Kaur [42]). At the same temperature, DEGME and DEGEE exhibited excellent consistency with previously published data, showing AADs of 0.15% (with Belhadj et al. [41]) and 0.13% (with Ouaar et al. [43]), respectively.

For the speed of sound, 1-HpOH again displayed very small deviations, with AADs of 0.07% at 303.15 K (with Aralaguppi and Baragi [40]) and 0.01% at 313.15 K (with Pina and Francesconi [44]). The results for DEGME and DEGEE also showed close agreement with literature, with respective AADs of 0.25% at 323.15 K (with Belhadj et al. [41]) and between 0.09% and 0.12% across the studied temperatures (with Ouaar et al. [43]). Similarly, EGPhE data were highly consistent

Table 10
Pure component data for the Peng-Robinson EoS [30].

Compound *	T_c [K]	P_c [bar]	ω
DEGME	630	35.45	0.635
DEGEE	656	30.53	0.7
EGME	564	50.84	0.387
EGPhE	698.15	36	0.806
EGBE	633.9	32.7	0.521
1-HpOH	632.6	30.58	0.567

* DEGME: Diethylene glycol monomethyl ether; DEGEE: Diethylene glycol monoethyl ether; EGME: Ethylene glycol monomethyl ether; EGPhE: Ethylene glycol monophenyl ether; and EGBE: Ethylene glycol monobutyl ether.

with Makhlouf et al. [17], yielding an AAD of 0.03% at 293.15 K. However, no comparative data were available in the literature for EGME and EGBE.

The refractive index measurements also confirmed the reliability of the present experimental dataset, as reflected by the low AAD values. Excellent agreement was achieved for DEGME (0.01%, with Belhadj et al. [41]) and DEGEE (0.006%, with Ouaar et al. [43]) at 293.15 K. For EGME, the deviations remained within 0.005% (with Lifi et al. [15]) at 293.15 K and 0.15% (with Jeevanandham et al. [45]) at 303.15 K, while EGPhE indicated an AAD of 0.02% (with Makhlouf et al., 2019 [17]). For EGBE, the deviation was slightly higher 0.10% at 303.15 K (with Jeevanandham et al. [45]). No reference data for 1-HpOH refractive indices at the studied temperatures were found.

To the best of our knowledge, no thermophysical data for the binary mixtures investigated here have been previously reported, underlining both the novelty and the significance of this contribution.

5.3. *Derivative properties*

Derived properties such as k_s, V^E and Δn_D of mixtures: x_1 DEGME + (1- x_1) 1-HpOH; x_1 DEGEE + (1- x_1) 1-HpOH; x_1 EGME + (1- x_1) 1-HpOH; x_1 EGPhE + (1- x_1) 1-HpOH and x_1 EGBE + (1- x_1) 1-HpOH, were adjusted along 293.15 K to 323.15 K, while maintaining a constant pressure (0.1 MPa). The A_i values employed to fit k_s, V^E, and Δn_D of each investigated pairwise system using Ep. (20) are provided in Table S5.

- **isentropic compressibility, (k_s)**

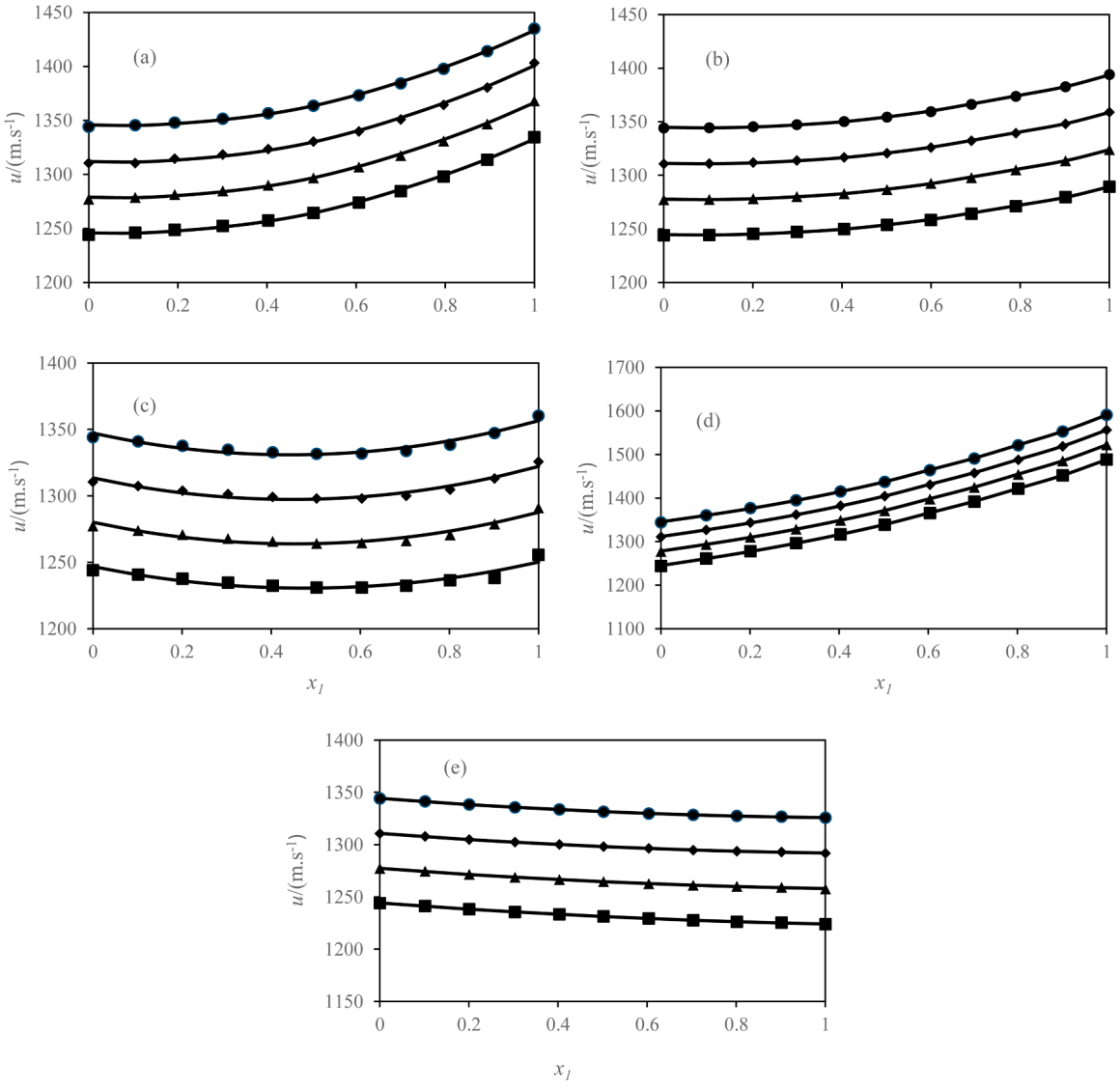

Fig. 4. Experimental values of speed of sound, u, as a function of mole fraction of x_1 for binary mixtures: (a) DEGME + 1-HpOH; (b) DEGEE + 1-HpOH; (c) EGME + 1-HpOH; (d) EGPhE +1-HpOH l and (e) EGBE + 1-HpOH. At temperatures: ●, 293.15 K; ◊, 303.15 K; ▲, 313.15 K; □, 323.15 K. (——), calculated values of refractive index with the polynomial equation (Eq. (22)).

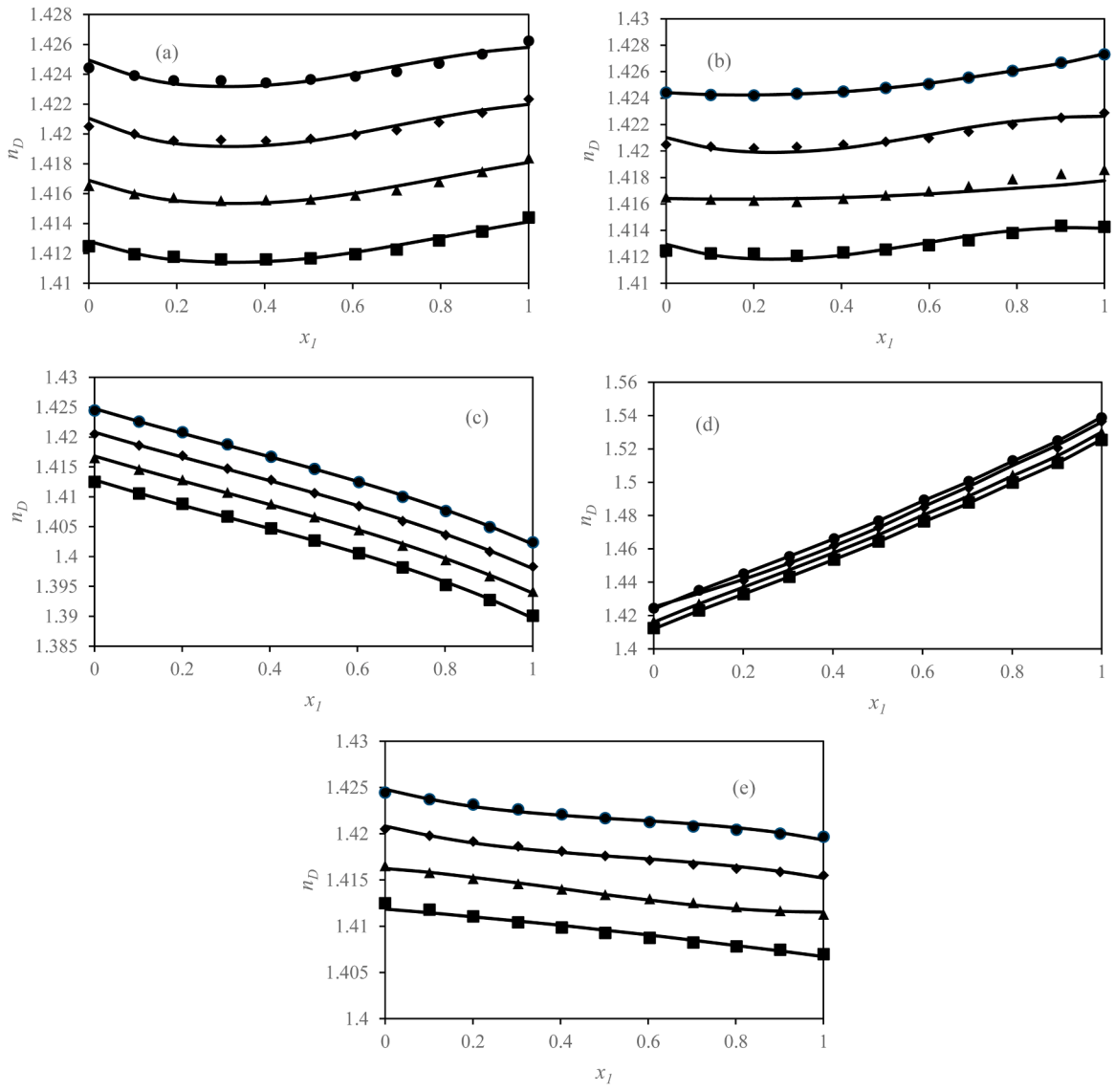

Fig. 5. Experimental values of refractive index, n_D, as a function of mole fraction of x_1 for binary mixtures (a) DEGME + 1-HpOH; (b) DEGEE + 1-HpOH; (c) EGME + 1-HpOH; (d) EGPhE +1-HpOH l and (e) EGBE + 1-HpOH. At temperatures: ●, 293.15 K; ◇, 303.15 K; ▲, 313.15 K; □, 323.15 K. (——), calculated values of refractive index with the polynomial equation (Eq. (22)).

Fig. 6 presents the variation of k_s, as a function of the mole composition x_1 for a series of binary systems involving alcohol and ether components. In all cases, k_s displays a non-linear dependence on fraction, indicative of notable molecular interactions within the mixtures. Frequently, a minimum compressibility arises at intermediate mole fractions, suggesting enhanced associative forces, notably hydrogen bonding or molecular association among the components.

This decrease in compressibility indicates a reduction in molecular free volume and a tighter structural arrangement within the liquid. As the temperature rises, compressibility generally increases, which is consistent with the weakening of intermolecular attractions and the greater average separation between molecules. The experimental results are accurately reproduced by the applied polynomial adjustment, as shown by the close match among the experimental data and the adjusted plots. This strong agreement confirms the reliability of the empirical expression in representing the variation of k_s over the investigated temperature and composition ranges.

Isentropic compressibility was calculated from density and speed of sound measurements; therefore, its uncertainty mainly reflects the uncertainties of these primary experimental quantities, and separate deviation values were not reported.

- **Excess molar volume, (V^E)**

Fig. 7 displays the variation in V^E for binary mixtures of selected glycol ethers with 1-HpOH, across different temperatures and mole fractions. The trends observed (see Fig. 7) emphasize the interplay between intermolecular forces and geometric compatibility within the mixtures.

Within the mixtures examined, the EGME + 1-HpOH system exhibits a particularly distinctive behavior. At 293.15 K and 303.15 K, the positive V^Evalues indicate a volume expansion upon mixing, which can be explained by the disruption of strong self-associative hydrogen bonds that dominate in the unmixed substances. At 313.15 K, however, the V^Evalues become negative, implying that stronger hetero-interactions form between EGME and 1-HpOH molecules, promoting closer molecular packing and resulting in a slight volume contraction. As the temperature rises further to 323.15 K, this compressive effect diminishes, and the V^Evalues return positive, reflecting a weakening of these interactions and an increase in molecular spacing.

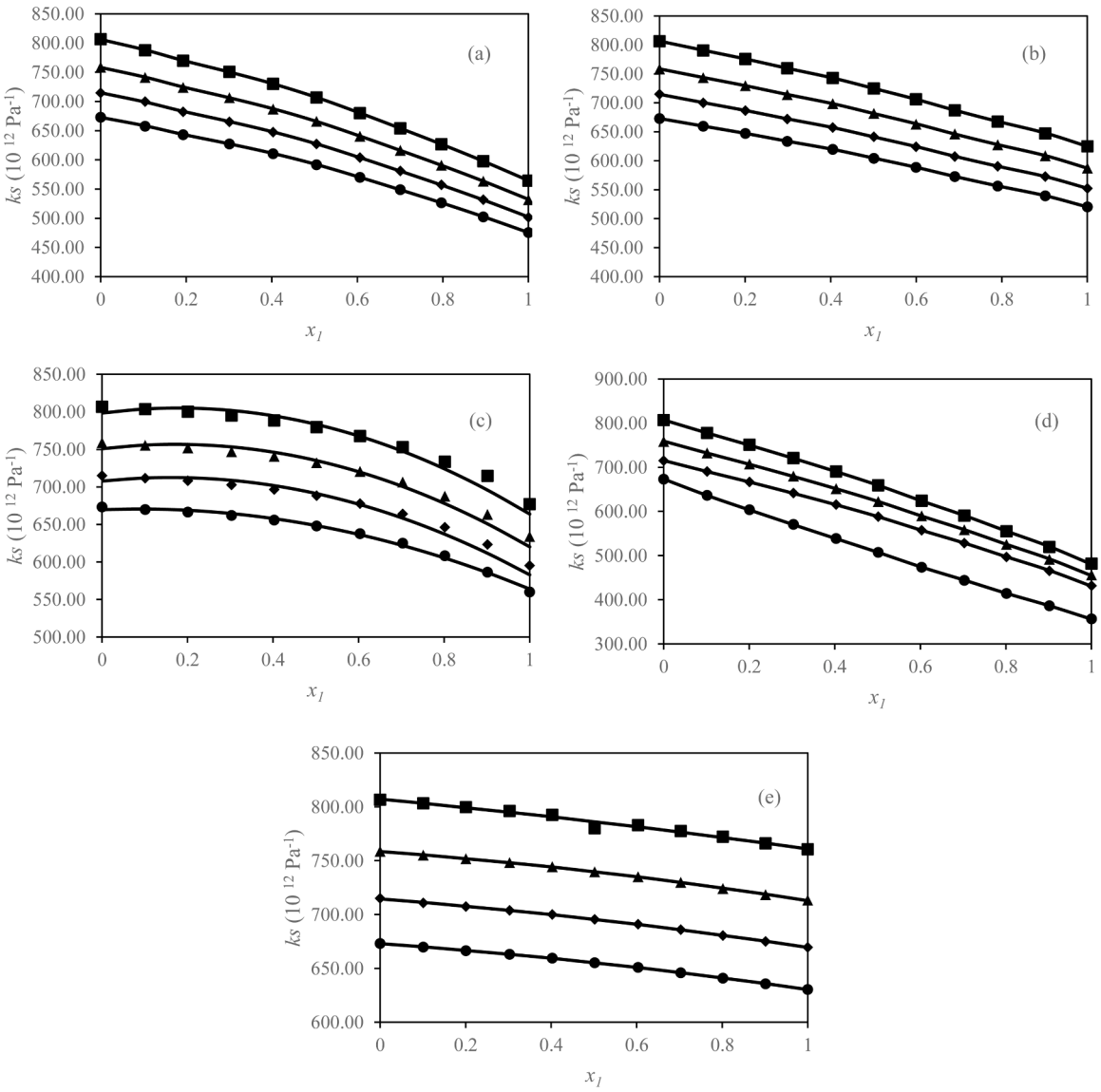

Fig. 6. Calculated values of isentropic compressibility, κ_S, as a function of mole fraction of x_1 for binary mixtures: (a) DEGME + 1-HpOH; (b) DEGEE + 1-HpOH; (c) EGME + 1-HpOH; (d) EGPhE +1-HpOH l and (e) EGBE + 1-HpOH. where: ●, 293.15 K; ◊, 303.15 K; ▲, 313.15 K; □, 323.15 K. (solid line) Calculated values of isentropic compressibility with the polynomial equation (eq 22).

In contrast, the mixtures of DEGME, DEGEE, EGPhE, and EGBE with 1-HpOH exhibit consistently negative V^E at all temperatures and compositions. This uniform contraction upon mixing reflects strong associative interactions mainly dipole–dipole attractions between dissimilar molecules and hydrogen bonding. Such interactions promote more efficient molecular packing, leading to a reduction in free volume.

The V^E curves are typically smooth and nearly symmetric, with noticeable minima appearing close to equimolar compositions ($x_1 \approx 0.5$), indicating a balanced contribution from both components during mixing. In systems containing larger or more rigid molecules, such as EGPhE, a slight asymmetry may arise due to disparities in the spatial dimensions of the molecule, geometry, and interaction potential, which subtly affect the overall volumetric behavior.

Temperature has a clear impact on these systems: as it increases, the magnitude of both expansion and contraction effects decreases, emphasizing the thermal sensitivity of intermolecular interactions. Overall, the findings highlight the key role of molecular structure and the nature of specific interactions in shaping the mixing behavior and V^E trends of glycol ether + 1-HpOH binary mixtures.

- **Deviation in refractive index, (Δn_D)**

The Δn_D for the binary systems of studied glycol ethers with 1-HpOH, was calculated according to:

$$\Delta n_D = n_D - \sum_{i+1}^{N} x_i n_{Di} \tag{25}$$

where n_D denotes the experimentally obtained refractive index of the mixture, x_i is the mole fraction of component i, and n_{Di} corresponds to the n_D of the unmixed component. As shown in Fig. 8, the calculation curves highlight a clear sensitivity to both temperature and molecular structure.

Generally, Δn_D increases with temperature across most compositions, indicating enhanced non-ideal behavior as thermal energy disrupts specific interactions within the mixtures. The maximum deviations are typically observed near equimolar compositions, reflecting strong interactions between dissimilar molecules that deviate significantly from ideal mixing.

DEGEE and EGBE both containing longer alkyl chains exhibit

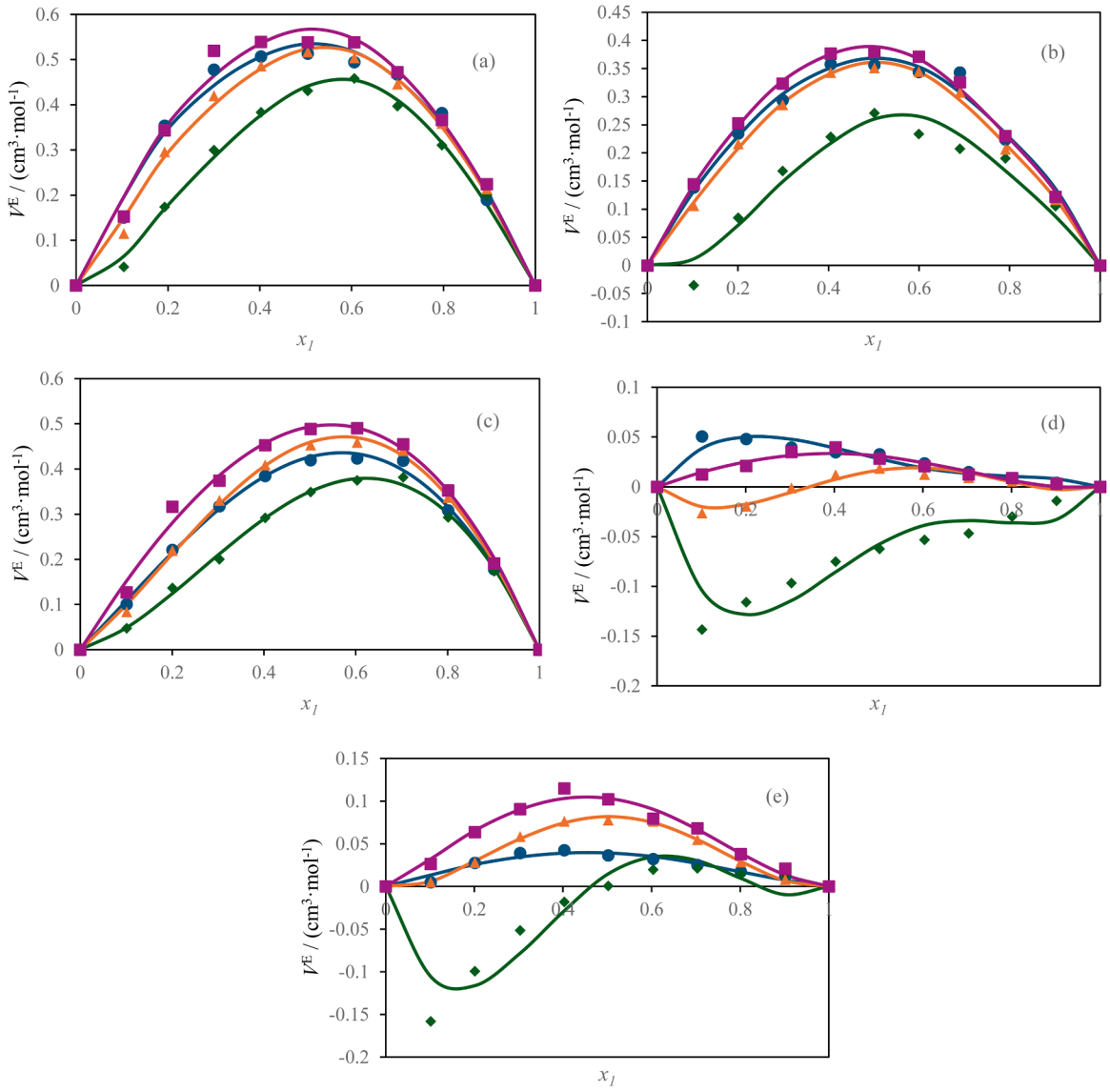

Fig. 7. Tendency curves of calculated values of excess molar volumes for the mixtures: (a) DEGME + 1-HpOH; (b) DEGEE + 1-HpOH; (c) EGME + 1-HpOH; (d) EGPhE +1-HpOH l and (e) EGBE + 1-HpOH as a function of the mole fraction, where: ●, 293.15 K; ◊, 303.15 K; ▲, 313.15 K; □, 323.15 K. Calculated values of excess volume with the Redlich-Kister equation (Eq. (21)) are presented by solid lines (—).

broader and more pronounced peaks in Δn_D. This suggests a greater extent of structural and electronic dissimilarity between these glycol ethers and 1-HpOH, leading to stronger perturbation of the original molecular interactions and increased deviation from ideality.

Conversely, systems incorporating shorter or more polar glycol ethers such as DEGME and EGME display narrower and less intense curves. This behavior points to more compatible interactions with 1-HpOH, resulting in more moderate deviations from ideal mixing.

A particularly notable trend is observed in the EGPhE + 1-HpOH system. Due to the presence of both polar functionalities and a bulky aromatic ring, this mixture exhibits a strong temperature dependence and noticeable asymmetry in the Δn_D curves. These features imply complex interactions involving both hydrophobic and polar components, which are highly sensitive to thermal effects.

Overall, the applied model effectively captures the main experimental trends, including the role of molecular dimensions, polarity, and interaction strength. These findings highlight the model's reliability for describing the refractive index deviation in structurally diverse binary systems.

6. Conclusions

This study examines the thermal and physical behavior of mixtures consisting of 1-heptanol and different glycol ethers over a range of temperatures. Experimental measurements of H_m^E, ρ, u and n_D were used to derive key excess properties, including the k_s, V^E and Δn_D. The resulting data were interpreted using both R–K equation and polynomial expressions to capture their composition-dependent variations. Density measurements were examined using conventional polynomial regressions and also through predictive approaches based on PC-SAFT and Peng–Robinson equations of state. Furthermore, excess molar enthalpy was interpreted with well-established thermodynamic frameworks NRTL, UNIQUAC, and DM-UNIFAC to better understand the molecular interactions governing the mixtures. By integrating experimental observations with empirical correlations and theoretical modeling, this study provides a comprehensive understanding of the non-ideal mixing behavior of these systems, highlighting their potential importance in renewable fuel development and bio-based component applications.

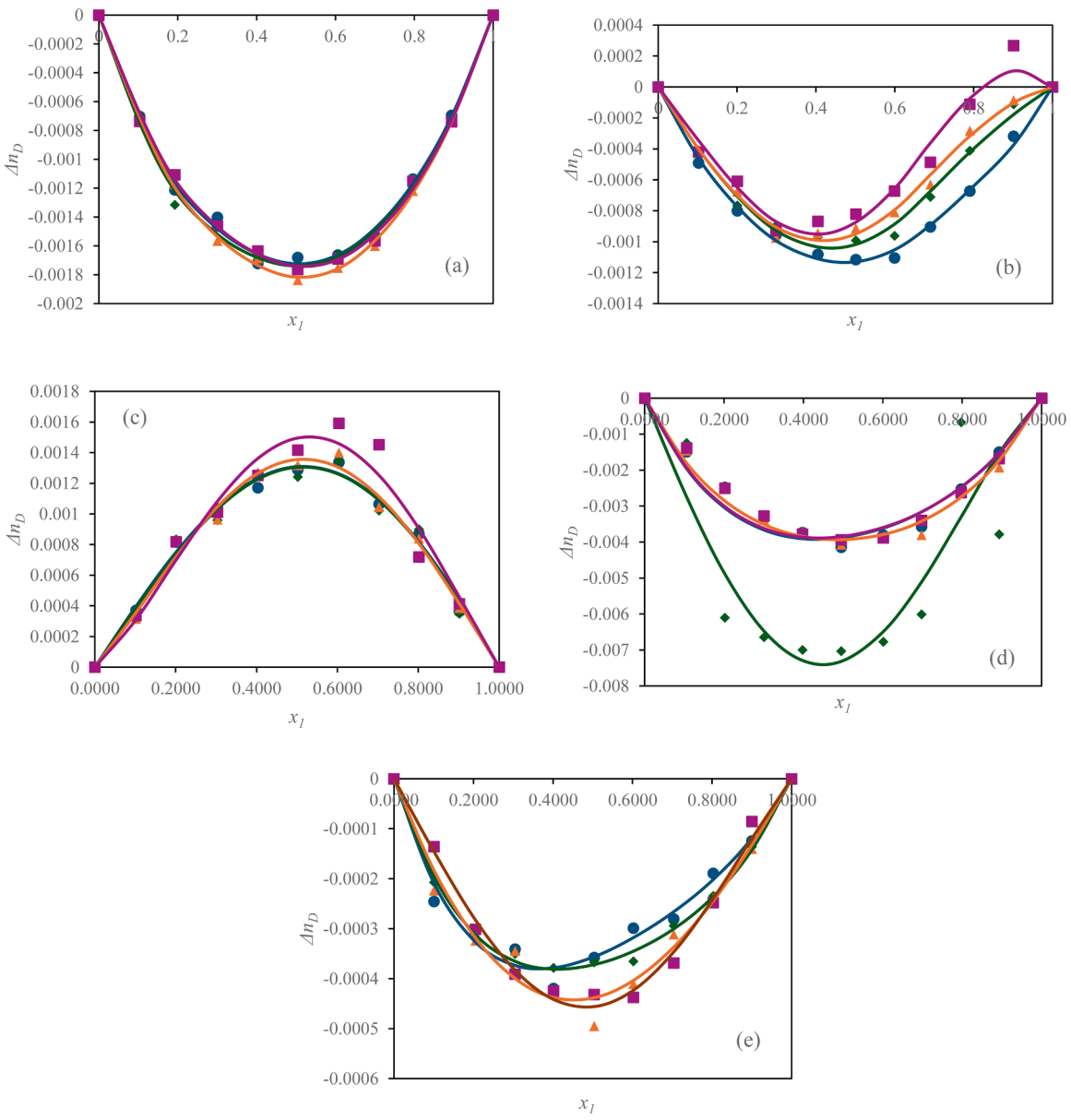

Fig. 8. Calculated values of Δn_D as a function of x_1 for: (a) DEGME + 1-HpOH; (b) DEGEE + 1-HpOH; (c) EGME + 1-HpOH; (d) EGPhE +1-HpOH l and (e) EGBE + 1-HpOH. At temperatures: ●, 293.15 K; ◊, 303.15 K; ▲, 313.15 K; □, 323.15 K. Calculated values of Δn_D with Eq. 21: (——), at 293.15 K, (——), at 303.15 K, (——), at 313.15 K and (——), at 323.15 K.

CRediT authorship contribution statement

Khaoula Samadi: Writing – original draft, Software, Investigation, Formal analysis. **Mohamed Lifi:** Writing – review & editing, Validation, Supervision, Software, Investigation, Formal analysis. **Houda Lifi:** Supervision, Investigation. **Mohamed Ouakarrouch:** Supervision, Investigation. **Fernando Aguilar:** Validation, Supervision. **Fatima Ezzahrae M'hamdi Alaoui:** Validation, Supervision.

Declaration of competing interest

The authors declare that they have no known competing financial interests or personal relationships that could have appeared to influence the work reported in this paper.

Supplementary materials

Supplementary material associated with this article can be found, in the online version, at doi:10.1016/j.tca.2026.180259.

Data availability

No data was used for the research described in the article.

References

[1] M.Y. Raza, W. Wang, Q. Javed, Decoupling Effect and Driving Factors of Transport CO2 Emissions: Modeling and Prediction of Energy and Environmental Factors towards Vision-2035 in a Developing Economy, Energy Strategy Rev 59 (2025) 101750, https://doi.org/10.1016/j.esr.2025.101750.
[2] H.K. Jeswani, A. Chilvers, A. Azapagic, Environmental Sustainability of Biofuels: A Review, Proc. R. Soc. Math. Phys. Eng. Sci. 476 (2243) (2020), https://doi.org/10.1098/rspa.2020.0351.
[3] M.H. Khademi, M. Lotfi-Varnoosfaderani, Use of Biomass-Derived Glycerol as an Alternative to Fossil Fuels for Aniline Production: Energy Saving and Environmental Aspects, Fuel 310 (2022) 122359, https://doi.org/10.1016/j.fuel.2021.122359.
[4] S. Zhao, R. Xu, X. Liu, Y. Wang, Y. Jiang, Effect of Carbon Chain Length and Concentration of Perfluorinated Compounds on Polytetrafluoroethylene

Microplastics Transport Behavior, NanoImpact 37 (2025) 100550, https://doi.org/10.1016/j.impact.2025.100550.
[5] J.A. González, I. Mozo, I. García De La Fuente, J.C. Cobos, N. Riesco, Thermodynamics of (1-Alkanol+linear Monoether) Systems, J. Chem. Thermodyn. 40 (10) (2008) 1495–1508, https://doi.org/10.1016/j.jct.2008.06.001.
[6] S. Karlapudi, R.L. Gardas, P. Venkat Eswarlu, K. Sivakumar, FT-IR Studies on Excess Thermodynamic Properties of Binary Liquid Mixtures o-Chlorotoluene with 1-Propanol, 1-Butanol, 1-Pentanol, 1-Hexanol and 1-Heptanol at Different Temperatures, J. Chem. Thermodyn. 67 (2013) 203–209, https://doi.org/10.1016/j.jct.2013.08.013.
[7] K.B. Bhumula, G.N. Kumar, Effect of Fuel Injection Timing on Engine Characteristics with an Equal Volume of 1-Heptanol/Diesel Blend in a CRDI CI Engine, Results Eng 26 (2025) 104632, https://doi.org/10.1016/j.rineng.2025.104632.
[8] Y. Yang, H. Zhou, J. Yao, R. Hong, W. Dong, B. Qiu, H. Chu, Effect of Long Chain Oxygenated Fuel on Soot Formation in N-Heptane Flames: An Experimental Study, J. Energy Inst. 119 (2025) 101984, https://doi.org/10.1016/j.joei.2025.101984.
[9] B.S. Chauhan, R.K. Singh, H.M. Cho, H.C. Lim, Practice of Diesel Fuel Blends Using Alternative Fuels: A Review, Renew. Sustain. Energy Rev. 59 (2016) 1358–1368, https://doi.org/10.1016/j.rser.2016.01.062.
[10] K. Samadi, M. Lifi, I. Abala, N. Muñoz-Rujas, F.E. M'hamdi Alaoui, F. Aguilar, Thermophysical Analysis and Molecular Modeling of 2-Propanol–Glycol Ether Mixtures Between 293.15 K and 323.15 K: Implications for Renewable Fuel Formulations, Int. J. Thermophys. 46 (2025) 147, https://doi.org/10.1007/s10765-025-03616-3.
[11] P.J. Carvalho, C.H.G. Fonseca, M.-L.C.J. Moita, Â.F.S. Santos, J.A.P. Coutinho, Thermophysical Properties of Glycols and Glymes, J. Chem. Eng. Data 60 (12) (2015) 3721–3737, https://doi.org/10.1021/acs.jced.5b00662.
[12] F. Gómez-Cuenca, M. Gómez-Marín, M.B. Folgueras-Díaz, Effects of Ethylene Glycol Ethers on Diesel Fuel Properties and Emissions in a Diesel Engine, Energy Convers. Manag. 52 (8–9) (2011) 3027–3033, https://doi.org/10.1016/j.enconman.2011.04.017.
[13] F.P. Chegini, H. Iloukhani, Kh. Khanlarzadeh, The Study of Thermodynamic Properties of Diethylene Glycol Monoethyl Ether with 2-Alkanols (C3 − C7) with Use of PFP and ERAS Modeling, J. Chem. Thermodyn. 201 (2025) 107392, https://doi.org/10.1016/j.jct.2024.107392.
[14] S. Ganji, T.S. Krishna, D. Venkatesan, R. Day, D. Ramachandran, Thermodynamic and Transport Properties of Binary Mixtures Containing 1,2-Propanediol with 2-Methoxyethanol and 2-Ethoxyethanol at Different Temperatures, J. Chem. Thermodyn. 201 (2025) 107396, https://doi.org/10.1016/j.jct.2024.107396.
[15] M. Lifi, I. Abala, N. Munoz-Rujas, F. Aguilar, E.A. Montero, L. Negadi, F. E. M'hamdi Alaoui, Thermophysical Properties of Binary Liquid Mixtures of Oxygenated Compounds: 2-Methoxyethanol + Alcohols at T = 298.15 K and 313.15 K, J. Chem. Thermodyn. 164 (2022) 106593, https://doi.org/10.1016/j.jct.2021.106593.
[16] V. Alonso, M. García, J.A. González, I. García De La Fuente, J.C. Cobos, Thermodynamics of Mixtures Containing Alkoxyethanols. XXVIII: Liquid–Liquid Equilibria for 2-Phenoxyethanol+selected Alkanes, Thermochim. Acta 521 (1–2) (2011) 107–111, https://doi.org/10.1016/j.tca.2011.04.012.
[17] H. Makhlouf, N. Muñoz-Rujas, F. Aguilar, B. Belhachemi, E.A. Montero, I. Bahadur, L. Negadi, Density, Speed of Sound and Refractive Index of Mixtures Containing 2-Phenoxyethanol with Propanol or Butanol at Various Temperatures, J. Chem. Thermodyn. 128 (2019) 394–405, https://doi.org/10.1016/j.jct.2018.08.029.
[18] C.M. Kinart, M. Maj, A. Ćwiklińska, W.J.Densities Kinart, Viscosities and Relative Permittivities of Some n-Alkoxyethanols with Sulfolane at T=303.15 K, J. Mol. Liq. 139 (1–3) (2008) 1–7, https://doi.org/10.1016/j.molliq.2007.10.003.
[19] O. Redlich, A.T. Kister, Algebraic Representation of Thermodynamic Properties and the Classification of Solutions, Ind. Eng. Chem. 40 (2) (1948) 345–348, https://doi.org/10.1021/ie50458a036.
[20] D.S. Abrams, J.M. Prausnitz, Statistical Thermodynamics of Liquid Mixtures: A New Expression for the Excess Gibbs Energy of Partly or Completely Miscible Systems, AIChE J. 21 (1) (1975) 116–128, https://doi.org/10.1002/aic.690210115.
[21] M.M. Abbott, H.C. Van Ness, Vapor-liquid Equilibrium: Part III. Data Reduction with Precise Expressions for G^E, AIChE J 21 (1) (1975) 62–71, https://doi.org/10.1002/aic.690210107.
[22] U. Weidlich, J. Gmehling, A Modified UNIFAC Model. 1. Prediction of VLE, hE, and .Gamma..Infin, Ind. Eng. Chem. Res. 26 (7) (1987) 1372–1381, https://doi.org/10.1021/ie00067a018.
[23] J. Gross, G. Sadowski, Perturbed-Chain SAFT: An Equation of State Based on a Perturbation Theory for Chain Molecules, Ind. Eng. Chem. Res. 40 (4) (2001) 1244–1260, https://doi.org/10.1021/ie0003887.
[24] F. Aguilar, F.E.M. Alaoui, C. Alonso-Tristán, J.J. Segovia, M.A. Villamañán, E. A. Montero, Excess Enthalpies of Binary and Ternary Mixtures Containing Dibutyl Ether, Cyclohexane, and 1-Butanol at 298.15 K, J. Chem. Eng. Data 54 (6) (2009) 1672–1679, https://doi.org/10.1021/je800751m.
[25] EA 4/02: Expression of the Uncertainty of Measurement in Calibration, European co-operation for Accreditation, Paris, 1999.
[26] J. Gmehling, J. Li, M. Schiller, A Modified UNIFAC Model. 2. Present Parameter Matrix and Results for Different Thermodynamic Properties, Ind. Eng. Chem. Res. 32 (1) (1993) 178–193, https://doi.org/10.1021/ie00013a024.
[27] J. Gross, G. Sadowski, Application of the Perturbed-Chain SAFT Equation of State to Associating Systems, Ind. Eng. Chem. Res. 41 (22) (2002) 5510–5515, https://doi.org/10.1021/ie010954d.
[28] I. Abala, M. Lorenzo-Bañuelos, H. Lifi, M. Lifi, N. Muñoz-Rujas, F. Aguilar, M'hamdi Alaoui, F.E. Density, Viscosity, Refractive Index, and Related Thermophysical Properties of Dibutyl Ether +2-Butanol + Cyclohexane Ternary Systems, J. Chem. Eng. Data 67 (12) (2022) 3532–3542, https://doi.org/10.1021/acs.jced.2c00298.
[29] I. Abala, M. Lifi, Y. Chhiti, R.A. Belale, F.E.M. Alaoui, M.E. Khouakhi, L. Deshayes, Estimation of PC-SAFT Equation of State Parameters of Hydrocarbons, Alcohols and Ethers, in: 2020 5th International Conference on Renewable Energies for Developing Countries (REDEC), IEEE, Marrakech, Morocco, Morocco, 2020, pp. 1–6, https://doi.org/10.1109/redec49234.2020.9163834.
[30] Critical Properties and Acentric Factor—Organic Compounds, Thermophysical Properties of Chemicals and Hydrocarbons, Elsevier, Amsterdam, 2014.
[31] M. Škerget, Z. Novak-Pintarič, Ž. Knez, Z. Kravanja, Estimation of Solid Solubilities in Supercritical Carbon Dioxide: Peng–Robinson Adjustable Binary Parameters in the near Critical Region, Fluid Phase Equilibria 203 (1–2) (2002) 111–132, https://doi.org/10.1016/S0378-3812(02)00177-2.
[32] H. Renon, J.M. Prausnitz, Local Compositions in Thermodynamic Excess Functions for Liquid Mixtures, AIChE J 14 (1) (1968) 135–144, https://doi.org/10.1002/aic.690140124.
[33] P.R. Bevington, D.K. Robinson, Data Reduction and Error Analysis for the Physical Sciences, WCD/McGraw-Hill, Boston, 1992.
[34] S. Verma, P. Bhagat, S. Gahlyan, M. Rani, N. Kumar, R.K. Malik, Y. Lee, S. Maken, Thermophysical Properties of 2-Amino-2-Methylpropan-1-Ol + Alkanol Mixtures: Investigation of Molecular Interactions by Insight of FT-IR Spectroscopy, J. Mol. Liq. 382 (2023) 121967, https://doi.org/10.1016/j.molliq.2023.121967.
[35] S. Verma, K. Kumari, S. Gahlyan, J.H. Kim, J. Min, S.Volumetric Maken, FT-IR, and Optical Properties of 2–Amino-1-Butanol with Isomeric Butanol at 298.15 K–318.15 K Using PFP Theory and Graph Theoretical Approach, J. Chem. Thermodyn. 209 (2025) 107524, https://doi.org/10.1016/j.jct.2025.107524.
[36] I. Abala, F.E. M'hamdi Alaoui, Y. Chhiti, A. Sahib Eddine, N. Munoz Rujas, F. Aguilar, Experimental Density and PC-SAFT Modeling of Biofuel Mixtures (DBE + 1-Heptanol) at Temperatures from (298.15 to 393.15) K and at Pressures up to 140 MPa, J. Chem. Thermodyn. 131 (2019) 269–285, https://doi.org/10.1016/j.jct.2018.11.010.
[37] S. Verma, K. Kumari, S. Gahlyan, S.J. Baek, J. Min, S. Maken, Investigation of Transport and Acoustic Properties of Binary Mixtures of 2–Amino–1–Butanol with Isomeric Butanol at 298.15 K–318.15 K: Graph Theoretical Approach and Bloomfield–Devan Model, J. Taiwan Inst. Chem. Eng. 170 (2025) 106001, https://doi.org/10.1016/j.jtice.2025.106001.
[38] I. Abala, M. Lifi, R. Briones-Llorente, H. Lifi, F. Aguilar, F.E. M'hamdi Alaoui, Temperature-Dependent Thermophysical Properties of 2-Propanol and Alkoxyethanol Mixtures: Insights from Experimental, Correlation, and Modeling Approaches, J. Chem. Eng. Data (2025), https://doi.org/10.1021/acs.jced.5c00171.
[39] F.E.M. Alaoui, E.A. Montero, G. Qiu, F. Aguilar, J. Wu, Liquid Density of Biofuel Mixtures: 1-Heptanol+heptane System at Pressures up to 140MPa and Temperatures from 298.15K to 393.15K, J. Chem. Thermodyn. 65 (2013) 174–183, https://doi.org/10.1016/j.jct.2013.05.051.
[40] M.I. Aralaguppi, J.G. Baragi, Physico-Chemical and Excess Properties of the Binary Mixtures of Methylcyclohexane+ethanol, +propan-1-Ol, +propan-2-Ol, +butan-1-Ol, +2-Methyl-1-Propanol, or 3-Methyl-1-Butanol at T=(298.15, 303.15, and 308.15)K, J. Chem. Thermodyn. 38 (4) (2006) 434–442, https://doi.org/10.1016/j.jct.2005.06.011.
[41] D. Belhadj, I. Bahadur, A. Negadi, N. Muñoz-Rujas, E. Montero, L. Negadi, Thermodynamic, Ultrasonic, and Transport Study of Binary Mixtures Containing 2-(2-Methoxyethoxy)Ethanol and Alcohols at (293.15–323.15) K, J. Chem. Eng. Data 65 (11) (2020) 5192–5209, https://doi.org/10.1021/acs.jced.0c00330.
[42] G.P. Dubey, P. Kaur, Thermodynamic and Spectral Investigations of Binary Liquid Mixtures of 2-Butoxy Ethanol with Alcohols at Temperature Range of 293.15–313.15K, Fluid Phase Equilibria 354 (2013) 114–126, https://doi.org/10.1016/j.fluid.2013.06.021.
[43] F. Ouaar, I. Mokbel, A. Negadi, F. Aguilar, E.A. Montero, J. Jose, I. Bahadur, L. Negadi, Vapor–Liquid Equilibria, Density, Sound Velocity, and Refractive Index for Binary Mixtures Containing 2-(2-Ethoxyethoxy)Ethanol and 1-Propanol or 2-Propanol or 1-Butanol or 2-Butanol at Different Temperatures, J. Chem. Eng. Data 65 (5) (2020) 2351–2372, https://doi.org/10.1021/acs.jced.9b00959.
[44] C.G. Pina, A.Z. Francesconi, New Applications of the ERAS-Model: Excess Volumes of Binary Liquid Mixtures of 1-Alkanols with Acetonitrile, Fluid Phase Equilibria 143 (1–2) (1998) 143–152, https://doi.org/10.1016/s0378-3812(97)00294-x.
[45] P. Jeevanandham, S. Kumar, P. Periyasamy, Densities, Viscosities, Refractive Indices and Excess Properties of Ortho- and Meta-Chloroaniline with 2-Alkoxyethanols at 303.15K, J. Mol. Liq. 188 (2013) 203–209, https://doi.org/10.1016/j.molliq.2013.09.035.
[46] H.A. Zarei, F. Jalili, Densities and Derived Thermodynamic Properties of (2-Methoxyethanol+1-Propanol, or 2-Propanol, or 1,2-Propandiol) at Temperatures from T=(293.15 to 343.15)K, J. Chem. Thermodyn. 39 (1) (2007) 55–66, https://doi.org/10.1016/j.jct.2006.06.001.